Title

Phenotypic and transcriptomic analyses reveal major differences between apple and pear scab nonhost resistance

Authors

Vergne E.[1*], Chevreau E.[1*], Ravon E.[1], Gaillard S.[1], Pelletier S.[1], Bahut M.[2], Perchepied L.[1]

Affiliations

[1] Univ Angers, Institut Agro, INRAE, IRHS, SFR QUASAV, F-49000 Angers, France

[2] Univ Angers, SFR QUASAV, F-49000 Angers, France

*E. Vergne and E. Chevreau made equal contributions to this work.

Corresponding author

E.Vergne

Emilie.vergne@inrae.fr

Abstract

Background. Nonhost resistance is the outcome of most plant/pathogen interactions, but it has rarely been described in Rosaceous fruit species. Apple (*Malus x domestica* Borkh.) have a nonhost resistance to *Venturia pyrina*, the scab species attacking European pear (*Pyrus communis* L.). Reciprocally, *P. communis* have a nonhost resistance to *Venturia inaequalis*, the scab species attacking apple. The major objective of our study was to compare the scab nonhost resistance in apple and in European pear, at the phenotypic and transcriptomic levels.

Results. Macro- and microscopic observations after reciprocal scab inoculations indicated that, after a similar germination step, nonhost apple/*V. pyrina* interaction remained nearly symptomless,

whereas more hypersensitive reactions were observed during nonhost pear/*V. inaequalis* interaction. Comparative transcriptomic analyses of apple and pear nonhost interactions with *V. pyrina* and *V. inaequalis*, respectively, revealed differences. Very few differentially expressed genes were detected during apple/*V. pyrina* interaction, preventing the inferring of underlying molecular mechanisms. On the contrary, numerous genes were differentially expressed during pear/*V. inaequalis* interaction, allowing a deep deciphering. Pre-invasive defense, such as stomatal closure, could be inferred, as well as several post-invasive defense mechanisms (apoplastic reactive oxygen species accumulation, phytoalexin production and alterations of the epidermis composition). In addition, a comparative analysis between pear scab host and nonhost interactions indicated that, although specificities were observed, two major defense lines seems to be shared in these resistances: cell wall and cuticle potential modifications and phenylpropanoid pathway induction.

Conclusion. This first deciphering of the molecular mechanisms underlying a nonhost scab resistance in pear offers new possibilities for the genetic engineering of sustainable scab resistance in this species. Concerning nonhost scab resistance in apple, further analyses must be considered with the aid of tools adapted to this resistance with very few cells engaged.

Keywords: apple, pear, nonhost resistance, transcriptomics

Background

Apple (*Malus x domestica* Borkh.) and European pear (*Pyrus communis* L.) are two closely related species belonging to the *Rosaceae* family. Reclassification of the *Rosaceae* placed both *Pyrus* and *Malus* genera in the subfamily *Spiraeoideae*, tribe *Pyreae* and subtribe *Pyrinae,* this subtribe corresponding to the long-recognized subfamily *Maloideae* [1]. Efforts to resolve relationships within this subtribe have frequently failed, and Campbell et al. [2] concluded that the genera of this subtribe *Pyreae* have not diverged greatly genetically. The recent sequencing of the pear genome [3] allowed a precise comparison with the apple genome [4] and led to the estimation of a divergence time

52 between the two genera of ≈ 5.4 – 21.5 million years ago. Furthermore, apple and pear genomes
53 share similar chromosome number (n=17), structure and organization.

54 Scab disease, caused by *Venturia* spp., affects several rosaceous fruit tree species. These
55 hemibiotrophic pathogens can infect only a limited host-range during their parasitic stage, but they
56 can overwinter as saprophytes in the leaf litter of a larger range of plant species [5]. Scab disease is
57 caused by *V. inaequalis* on apple, by *V. pyrina* (formerly named *V. pirina* [6]) on European pear, and
58 by *V. nashicola* on Japanese (*P. pyrifolia* Nakai) and Chinese (*P. ussuriensis* Maxim) pears. Cross
59 inoculations of *Venturia* spp. on different rosaceous fruit trees indicates that these pathogens are
60 highly host specific, probably indicating a close co-evolution of these pathogens with their hosts [7].
61 A plant species unable to be successfully infected by all isolates of a pathogen species is considered
62 as a nonhost for this pathogen. Nonhost interactions of *Venturia* spp. on apple and pear have rarely
63 been described. Microscopic observations have been made on *P. communis / V. nashicola* [8] as well
64 as *M. domestica* / *V. pyrina* and *P. communis* / *V. inaequalis* [5, 9]. In all cases, conidia germinated
65 and produced appressoria and runner hypheae, but failed to establish a network of stroma. No
66 macroscopic symptoms were visible.

67 Because of its durability, nonhost resistance has attracted numerous studies over the last
68 decade, which have uncovered its multiple and complex defense components. The underlying
69 mechanisms of nonhost resistance comprise pre-invasion resistance with preformed or induced cell-
70 wall defenses, metabolic defense with phytoanticipin or phytoalexin accumulation, pattern-triggered
71 immunity (PTI) as well as elicitor-triggered immunity (ETI) and various signaling pathways [10].

72 To our knowledge, the molecular bases of scab nonhost resistance of apple and pear have
73 never been investigated. We were not able to find reports on large-scale fungi nonhost resistance
74 analyses in pear and the few available in apple are about *Penicillium digitatum* and are conducted on
75 fruit [11, 12].

76 However, it is possible to find genome-wide molecular analyses of scab host resistance in
77 apple and pear. Thus, Perchepied et al. [13] performed a detailed transcriptomic analysis of the host

78 resistance of pear against *V. pyrina* strain VP102, deployed in a transgenic pear bearing the well-
79 known apple *Rvi6* resistance gene against *V. inaequalis*. They reported the modulation of expression
80 of 4170 genes and revealed that downstream of the pathogen recognition, the signal transduction
81 was triggered with calcium, G-proteins and hormonal signaling (jasmonic acid (JA) and
82 brassinosteroids), without involvement of salicylic acid (SA), and that this led to the induction of
83 defense responses such as a remodeling of primary and secondary cell wall, cutin and cuticular waxes
84 biosynthesis, systemic acquired resistance (SAR) signal perception in distal tissues, and the
85 biosynthesis of phenylpropanoids (flavonoids and lignin). Only four other transcriptomic studies
86 involving pear/pathogen host interactions have been published so far but are not concerning scab.
87 Yan et al. [14] reported the modulation of expression of 144 pear genes after fruit treatment by
88 *Meyerozyma guilliermondii*, an antagonistic yeast used for biocontrol of natural pear fruit decay.
89 Zhang et al. [15] similarly reported the modulation of expression of 1076 pear genes after treatment
90 with *Wickerhamomyces anomalus*, another biocontrol agent. Using RNA-seq, Wang et al. [16]
91 reported a major role of ethylene signalization during the compatible interaction between *P. pyrifolia*
92 and *Alternaria alternata*, a necrotrophic pathogen. Finally, Xu et al. [17] applied RNA-seq to
93 characterize the genes of *Penicillium expansum* activated after infection of pear fruits.

94 Concerning host resistance of apple against *V. inaequalis*, subtractive hybridization [18, 19]
95 and cDNA-AFLP [20] led to the identification of a limited set of differentially expressed genes in *Rvi6*
96 natural resistant 'Florina' variety (scab inoculated 'Florina' versus mock, [19]), or in *Rvi6* resistant
97 transgenic 'Gala' lines (*Rvi6* transgenic 'Gala' versus non-transformed 'Gala', after scab inoculation,
98 [18]; *Rvi6* transgenic 'Gala' before versus post scab inoculation, [20]). Recently, Perchepied et al. [13]
99 also performed a transcriptomic analysis of the *Rvi6* resistance in a transgenic 'Gala' line (transgenic
100 versus non-transformed, before and after scab inoculation). They reported the modulation of
101 expression of 2977 genes and revealed that downstream of the pathogen recognition, signal
102 transduction was triggered with calcium and interconnected hormonal signaling (auxins and
103 brassinosteroids), without involvement of SA, and that this led to the induction of defense responses

104 such as a remodeling of primary and secondary cell wall, galactolipids biosynthesis, SAR signal
105 generation and the biosynthesis of flavonoids. Genome-wide molecular analyses of apple scab host
106 resistance have also been achieved in other context than the *Rvi6* resistance. A RNA-seq analyze
107 identified five candidate genes putatively involved in the ontogenic scab resistance of apple [21]. In
108 addition, nuclear proteome analysis identified 13 proteins with differential expression patterns
109 among varying scab resistance 'Antonovka' accessions [22]. Recently, Masoodi et al. [23] performed
110 a RNA-seq analyze comparing three scab-resistant ('Florina', 'Prima', and 'White Dotted Red') and
111 three susceptible ('Ambri', 'Vista Bella', and 'Red Delicious') apple genotypes out to mine new scab
112 resistance genes. They reported the modulation of expression of 822 genes related to various
113 pathways, i.e., metabolic, protein processing, biosynthesis of secondary metabolites, plant hormone
114 signal transduction, autophagy, ubiquitin-mediated proteolysis, plant-pathogen interaction, lipid
115 metabolism, and protein modification pathways.

116 Thus, if large-scale analyses of pear and apple scab host resistance can be found, in-depth
117 knowledge of transcriptional patterns and gene functions involved in apple and pear scab nonhost
118 resistance is still needed. The objectives of our study were 1) to precisely describe nonhost resistance
119 symptoms in *M. domestica* / *V.pyrina* and *P. communis* / V. *inaequalis* interactions 2) to analyze the
120 underlying molecular mechanisms of both nonhost interactions through a transcriptomic study 3) to
121 compare the mechanism of host [13, 23] and nonhost scab resistance in apple and European pear.

122

123 Results

124 Macroscopic and microscopic symptoms analyze

125 Nonhost interactions were observed in a test performed on leaves of 'Gala' apple and
126 'Conference' pear cultivars, inoculated by a *V. pyrina* strain (VP102) and a *V. inaequalis* strain (VI
127 EUB05) respectively. At the macroscopic level, a total absence of sporulation was observed on all
128 nonhost interactions (Table 1), on the contrary to host interactions (Fig. 1 A and B). Very few pear
129 plants inoculated with *V. inaequalis* presented resistance symptoms such as pin points (Fig. 1C) and

130 chlorotic lesions (Fig. 1D), whereas the apple 'Gala' remained completely symptomless after *V. pyrina*

131 inoculations (Fig. 1E).

132

133 **Table 1: Scab qualitative note of pear and apple lines inoculated with *V. pyrina* and *V. inaequalis.***

Percentage (number) of plants in the different classes of symptoms, 42 days after inoculation				
Class of symptoms	*V. pyrina* strain VP102		*V. inaequalis* strain EUB05	
	'Conference'	'Gala'	'Conference'	'Gala'
0: absence of symptoms	0	100 (28)	90 (17)	0
1: hypersensitivity (pin points)	0	0	5 (1)	0
2: resistance (chlorotic lesions, slight necrosis, crinkled aspect)	0	0	5 (1)	0
3a: weak resistance (necrotic or chlorotic lesions with occasional very light sporulation)	0	0	0	0
3b: weak susceptibility (clearly sporulating chlorotic or necrotic lesions)	0	0	0	0
4: susceptibility (sporulation only)	100 (19)	0	0	100 (28)

134

135

136 At the microscopic level, three days after inoculation, there was no clear difference between

137 host and nonhost interactions: the conidia of *V. inaequalis* and *V. pyrina* germinated equally on both

138 hosts forming one or two appressoria (Fig. 1 F and G). However, 14 days after inoculation, there was

139 a clear reaction of the plant cells in contact with the appressoria (accumulation of red

140 autofluorescent compounds and enlargement of these cells), which could indicate very small scale

141 hypersensitive reactions (HR) (Fig. 1 H and I) in both plant species, more frequently in pear than in

142 apple (Fig1. J and K). No formation of subcuticular stroma and no conidiogenesis were observed in

143 the nonhost interactions.

144

145 Global gene expression analyze

146 Differentially expressed genes (DEGs) were obtained by comparing transcript abundance in

147 leaves between T0 and 24 hours post inoculation (hpi) and between T0 and 72 hpi, in the nonhost

148 interactions 'Gala' / *V. pyrina* VP102 and 'Conference' / *V. inaequalis* EUB05. These time points were
149 chosen in order to cover the period of establishment of the first intimate contacts between fungal
150 and plant cells: conidia germination and appressoria formation. For each comparison, the
151 experimental design is a dye switch approach [24] between the two biological repeats made by
152 condition (genotype x treatment x time). Each biological repeat is a pool of three leaves from three
153 different plants.

154 In total, 60 DEGs in apple and 1857 DEGs in pear were identified, which amounts to 0.19 % of
155 all apple genes on the apple AryANE v2.0 microarray, and 4.23 % of all pear genes on the Pyrus v1.0
156 microarray (Table 2). Among the 1857 pear DEGs, 80.2 % were only detected at 24 hpi and 15.4 %
157 only at 72 hpi, whereas 4.2 % were up-regulated or down- regulated similarly at both time points of
158 the experiment. Among all the pear DEGs observed at 24 and 72 hpi, the proportion of up-regulated
159 DEGs was higher (68.8 %) than the proportion of down-regulated DEGs (31.2 %).

160

161 **Table 2. Number of DEGs identified during apple and pear nonhost response to *V. pyrina* and *V.***
162 ***inaequalis***

	'Gala' / VP102		'Conference' / EUB05	
	24 hpi	72 hpi	24 hpi	72 hpi
Total # of DEGs*	49	11	1570	364
DEGs in % of all genes on the microarray**	0.16	0.03	3.58	0.83
% of up-regulated DEGs	67.3	36.4	74.5	25.5
% of down-regulated DEGs	32.7	63.6	25.5	74.5
% of DEGs without *Arabidopsis* homolog	27.1	30.4	0.70	1.09

163 *: DEGs numbers were calculated using the p-adj values ≤ 0.01 as selection threshold
164 **: 31311 genes on the apple Ariane V2 microarray, 43906 genes on the pear V1 microarray
165

166 To validate the transcriptomic data, 12 DEGs with varied ratios (between -1.9 and 2.9) were
167 tested by quantitative RT-PCR (qPCR; Table S1), on the two biological repeats used for transcriptomic
168 analyses. Considering the low number of DEGs found for apple in this study, we only tested two of
169 them in qPCR. As seen in Table 2 for pear, at 24 hpi, a majority of DEGs are up-regulated and at 72

170 hpi, a majority of DEG are down-regulated. qPCR was then performed essentially on DEGs with
171 positive ratios at 24 hpi and negative ratios at 72 hpi (Table S1). The qPCR results confirmed the
172 induced or repressed status of all tested DEGs.

173 Among the 1857 pear DEGs, the 1845 DEGs with *Arabidopsis* homologs (TAIR identifier) have
174 been classified according to MapMan functional categories (Fig. 2). In order to highlight the enriched
175 classes, the numbers of DEGs per category have been normalized to the numbers of *Arabidopsis*
176 genes in each MapMan category and bootstraps have been done to provide a confidence estimate
177 for the accuracy of the output (Fig. 2). We then more particularly explored the DEGs present in the
178 following enriched classes: Hormone metabolism, Stress, Lipid metabolism, Signaling, Secondary
179 metabolism, Cell wall, and depending on the defense pathways and responses identified, search for
180 others related DEGs in enriched wider classes: Protein, RNA and Miscellaneous. The Table 3 gives the
181 defense pathways and responses identified and the functional categories in which DEGs related to
182 these pathways/responses have been found. The analyze of the 184 DEGs found (corresponding to
183 158 different functions) is expanded in the Discussion section (Metadata of the 184 DEGs in Table
184 S2).

185

186 **Table 3. Numbers of DEGs in the defense pathways and responses identified among the enriched**
187 **functional categories analyzed in pear nonhost response to *V. inaequalis***

	Defense pathways and reponses identified												
MapMan functional categories	JA	SA/SAR	Calcium	ROS	Stomatal closure	HR	Cell Wall	Cuticle and waxes	Terpens and isoprenoids	Phenylpropanoids	Lignin	Coumarin and hydroxycinnamic acid	TOTAL
Protein	1					6						2	9
RNA	3					1		1		2			7
Miscellaneous		5				1		6			3	6	21
Hormone metabolism	10	2					1	1	3				17
Stress	4	11	2	1		3							21
Lipid Metabolism	5	1				8		7					21
Signalling		4	5	4	9	3							25
Secondary metabolism								4	9	5	11	2	31
Cell Wall							32						32
TOTAL	23	23	7	5	9	22	33	19	12	7	14	10	184

188

189 Among the 60 apple DEGs found, 17 have no *Arabidopsis* homolog, 12 more have
190 unpredicted function and for 11 more we could not find information (Metadata of the 60 DEGs in
191 Table S3). In view of our findings in pear / *V. inaequalis* nonhost interaction, 9 of the 20-remaining
192 apple DEGS could be relevant in apple / *V. pyrina* nonhost interaction and are further analyzed in the
193 Discussion section (Metadata of the 9 DEGs in Table S4).
194

195 **Discussion**

196 More frequent symptoms of nonhost resistance in pear versus apple at microscopic level

197 The apple 'Gala' remained completely symptomless after *V. pyrina* inoculations (Fig. 1E). This
198 is similar to the observation of Chevalier et al. [9] after inoculation of 'Gala' with another *V. pyrina*
199 strain. On the contrary, pear plants inoculated with *V. inaequalis* presented occasional pin points
200 symptoms (Fig. 1D) and chlorotic lesions (Fig. 1E). Chlorotic lesions had already been observed by
201 Chevalier et al. [9] after inoculation of the pear 'Pierre Corneille' with the *V. inaequalis* strain EUB04,
202 but pin points had never been reported in this nonhost interaction.
203

204 At the microscopic level, 14 days after inoculation, there was a clear reaction of the plant
205 cells in contact with the appressoria (accumulation of red autofluorescent compounds and
206 enlargement of these cells), which could indicate very small scale hypersensitive reactions (HR) (Fig. 1
207 H and I, I and K) in both plant species. No formation of subcuticular stroma and no conidiogenesis
208 were observed in the nonhost interactions, contrary to the host-resistance reactions [13]. These
209 observations are similar to the collapsed cells described by Chevalier et al. [9] in apple and pear
210 nonhost reactions, and to the rare HR-like reactions observed by Stehmann et al. [5] on apple
211 inoculated by *V. pyrina*.

212 Our results seems to indicate that the leaf surface morphology of apple and pear is equally
213 compatible with *V. pyrina* and *V. inaequalis* conidia germination, without specific inhibition at this
214 stage. Recognition probably occurs only at the appressorium site, leading to the cellular reactions

observed. These reactions were limited to a few cells without visible symptoms in apple / *V. pyrina* interaction, but more extended in pear / *V. inaequalis* interaction and could occasionally produce macroscopic symptoms.

Different patterns of global gene expression in nonhost resistance in pear versus apple

DEGs were analyzed by comparing transcript abundance in leaves between T0 and 24 hpi and between T0 and 72 hpi, in the nonhost interactions 'Gala' / *V. pyrina* VP102 and 'Conference' / *V. inaequalis* EUB05. This experimental design is open to criticism because it could include in results DEGs responding to the inoculation method (spray of water), and DEGs which expression varies due to leaves ageing. Water spray is effectively perceived as a mechanical stimulus by plants, the *Arabidopsis* response being largely regulated by the JA pathway induction under the control of MYC2/MYC3/MYC4 transcription factors [25]. But this response is transient and really fast as most of genes differentially regulated peak within 30 minutes regain untreated transcriptional levels within 3 hours [25]. It seems therefore very unlikely that our analysis at 24 and 72 hpi includes genes responding to water spray. Resistance due to leaves ageing i.e. ontogenic resistance has been investigated in *Malus-Venturia* pathosystem at 72 and 96 hpi, and 5 genes have been identified whose modulation could be linked to this resistance [21]. None of these apple genes, or homologs in pear, were found differentially expressed at 72 hpi in our interactions (Table S5), which argue against the presence of ageing responding genes in our results. In total, 60 DEGs in apple and 1857 DEGs in pear were identified, which amounts to 0.19 % of all apple genes on the apple AryANE v2.0 microarray, and 4.23 % of all pear genes on the Pyrus v1.0 microarray (Table 2).

The very small number of DEGs (60) detected in the apple/ *V. pyrina* nonhost interaction at 24 or 72 hpi seems in agreement with the total absence of macroscopic symptoms observed during this interaction, and the few small HR-like reactions detected at the microscopic level 14 days post inoculation. Because these reactions involve only a few cells in the leaves, the changes in gene

241 expression are probably below the threshold of DEG detection applied in this experiment. It is also
242 possible that the mild response of apple to *V. pyrina* occurs later than 72 hpi, between 72 hpi and 6
243 days after inoculation. Indeed, Chevalier et al. [9] observed these rare HR from 6 days post
244 inoculation, with no more evolution until 14 days after inoculation. A later time (6 days post
245 inoculation) would have been necessary to conclude on this last hypothesis.

246 On the contrary to apple/ *V. pyrina* nonhost interaction, the number of DEGs (1857) detected
247 during the pear / *V. inaequalis* interaction is in the same order of magnitude as the number of DEGs
248 detected during pear host resistance to *V. pyrina* (see [13]). This could be consistent with the more
249 frequent observation in this interaction of microscopic HR-like reactions detected 14 days post
250 inoculation, and of occasional macroscopic symptoms of resistance (chlorotic lesions or pin points).

251

252 Hormone signaling pathways classically associated to resistance seems weakly involved in pear / *V.*
253 *inaequalis* interaction

254 We found pear DEGs that seems to indicate that the JA pathway was repressed. The JA
255 biosynthesis and metabolic conversions were reviewed by Wasternack et al. [26]. In our data, at 24
256 hpi, the first step of JA biosynthesis, corresponding to the conversion of linoleic acid in 12-oxo-
257 phytodienoic acid (OPDA), seems to be compromised: six out of seven lipoxygenases (LOX) (three
258 LOX1, two LOX2 and two LOX5) are repressed, the last one being induced (Fig. 3). OPDA produced in
259 the chloroplast is then transported to the peroxisome for subsequent conversion to JA via the action
260 of OPR3 (12-oxo-phytodienoic acid reductase) and β-oxidation enzymes (reviewed in [27] and in
261 [26]). In pear, three β-oxidation enzymes were found activated more or less rapidly: ACX4 (24 hpi),
262 MFP2 (72 hpi) and the thioesterase homolog to *At2g29590* (72 hpi), which could suggest that
263 constitutive OPDA stocks were turned into JA. But the early and long-lasting induction of *JMT* and
264 *ST2A* genes could be in favor of a rapid conversion of JA in inactive compounds, *JMT* induction
265 potentially being reinforced by *BBD1* repression (24 hpi). *BBD1* is actually known as a negative
266 regulator of *JMT* [28].

267 The behavior of some DEGs seemed indicate that the defense response depending on JA was
268 also repressed in pear (Fig. 3). The transcription activator MYC2 of JA-induced genes is known to be
269 repressed by its interaction with JAZ proteins (reviewed in [26]), and two *JAZ1* and one *JAZ3* coding
270 genes were found activated at 24 hpi in pear. UBP12 is known as a stabilizer of MYC2 [29]. In our
271 data, *UBP12* was found repressed at 72 hpi, which could reinforce the inactivation of MYC2. WRKY33
272 is known as an activator of the JA defense pathway [30] and WRK70 [31] or AS1 (or MYB91; [32]) as
273 inhibitors, and among JA-responsive proteins, the pathogenesis-related PR3, PR4 and PR12 act
274 downstream MYC2 activation [33]. In our data, accordingly with the repression of the activator
275 WRKY33 and the activation of the inhibitors WRK70 and AS1, some JA-responsive genes were also
276 found repressed, such as the chitinase coding genes *PR4* (also called *HEL*) and *ATEP3*. Furthermore,
277 no DEGs were found for PR3 and PR12 functions. To conclude, in the nonhost interaction between
278 pear and *V. inaequalis*, some JA could be produced, but is rapidly converted into inactive compounds
279 and the subsequent defense response seems to be repressed.

280 Pear DEGs were found that could indicate that the SA pathway was slightly engaged and
281 rapidly repressed (Fig. 3). *WRKY70* was induced at 72 hpi in our data. This transcription factor is
282 known as a negative regulator of SA biosynthesis but a positive regulator of SA-mediated defense
283 genes in *Arabidopsis* [34, 35, 36], among them *PR2*, *PR5* but not *PR1* [37]. *WRKY33* which is known as
284 a negative regulator of SA-responsive genes [38], was also repressed at 72 hpi in our data. PR2 and 5
285 are well-known anti-fungal proteins [39, 40, 41]. At 24 hpi a *PR2*, two *PR2-like*, a *PR5* and a *PR5-like*
286 coding genes were found induced in our work, another *PR2-like* and two others *PR5-like* being
287 repressed. The differential expression was maintained at 72 hpi for only two of the previously
288 activated ones. Furthermore no DEG was found for the PR1 function but three *PR1-like* genes were
289 found repressed: *ATPRB1* and genes homolog to *At5g57625* and *At4g33720*. *ATPRB1* was already
290 reported as repressed by SA treatment [42]. In our data, the WRKY70 transcription factor was
291 induced later than the induced PR genes so we could imagine that induced PR genes were activated
292 by another precocious regulation, such as an oxidative burst (see below), rather than by WRKY70.

293 Furthermore, WRKY70 induction seems not sufficient to enable a long lasting induction of these
294 defense genes.

295 Other pear DEGs seems to indicate that SA accumulation was transient. *CBP60a* [43], *ACA11*
296 [44], *EICBP.B* (or *CATMA1*; [45]), all three coding calcium-sensor proteins, are known as negative
297 regulators of SA accumulation and biosynthesis, as well as the light signaling factor *FAR1* [46] or the
298 SA glucosyltransferase *UGT74F1* which convert SA in inactive SA 2-O-beta-D-glucoside or the glucose
299 ester of SA [47]. On the contrary *EDS1*, *PAD4* (reviewed in [48]) and *MKS1* [49] are known as positive
300 regulators of SA accumulation. In our data, the repression of *CBP60a*, *ACA11* and *EICBP.B* genes could
301 sustain a SA biosynthesis and accumulation. In addition, *EDS1* activation could allow to consider a
302 positive feedback loop likely to potentiate SA action via EDS1 cytosolic homodimers, even though
303 *PAD4* was repressed. But, as well as *WRKY70* induction, the repression of the MAPK *MKS1* and the
304 activation of the light signaling factor *FAR1* (2 times) or the SA glucosyltransferase *UGT74F1* could be
305 in favor of less free SA. Concerning SAR, *MES1* is known as required in healthy systemic tissues of
306 infected plants to release the active SA from methyl-SA, which serves as a long-distance signal for
307 SAR [48] and *ACBP6* may be involved in the generation of SAR inducing signal(s) [50]. In our data, SAR
308 seemed compromised given the repression of *ACBP6* at 24 hpi and *MES1* at 72 hpi. To conclude, in
309 the nonhost interaction between pear and *V. inaequalis*, the behavior of some DEGs led us to the
310 hypothesis that the SA pathway could be engaged but transiently and presumably reduced to the few
311 infection sites and not spread by SAR in healthy systemic tissues.

312

313 Calcium influx and reactive oxygen species (ROS) production seems to act as secondary messengers
314 and could lead to stomatal closure in pear / *V. inaequalis* interaction

315 Early responses of plants upon pathogen perception include calcium influx and ROS
316 production, which both act as secondary messengers ([51], reviewed in [10]). Three pear DEGs were
317 found that seems to indicate early increased cytosolic calcium level. The CSC (Calcium permeable
318 Stress-gated cation Channel) ERD4 (found two times) and the two glutamate receptors GLR3.4 and

319 GLR2.7, are known as calcium permeable channels [52, 53]. They were induced at 24 hpi in our data.
320 An increased cytosolic calcium level can lead to a pre-invasive defense response by stomatal closure
321 and promote the post-invasive defense response ROS accumulation [54].

322 Calcium influx has been reported to promote stomatal closure through the regulation of
323 potassium flux and the activation of anion channels in guard cells (reviewed in [10]). The stomata
324 closure is known to be induced via the inhibition of inward potassium currents which is achieved via
325 activation of calcium dependent protein kinases (CDPK) such as CPK13 and CPK8/CDPK19 [55, 56];
326 but also via activation of CBL1 of the CBL1-CIPK5 complex, which activates the GORK potassium
327 outward channel [57]. CPK13, CPK8/CDPK19 and CBL1 were all activated at 24 hpi in our data.

328 A NADPH oxidase *RBOHB* (respiratory burst oxidase homologs, RBOH) is early (i. e. 24 hpi)
329 and sustainably (through to 72 hpi) induced in the pear/*V. inaequalis* nonhost interaction, which
330 could suggest a rapid and maintained apoplastic ROS production. Indeed, the apoplastic ROS are
331 mainly produced by plasma membrane localized NADPH oxidases, cell wall peroxidases and amine
332 oxidases [58]. In addition, posttranslational regulation of RBOH is required for its activation and ROS
333 production. Calcium, phosphatidic acid, and direct interactors such as Rac1 GTPase and RACK1
334 (Receptor for Activated C-Kinase 1) have been reported to be positive regulators of RBOHs (reviewed
335 in [59]). For example, the Rac-like/ROP GTPase ARAC3 is known to interact with a RBOH to promote
336 ROS production [60]. In our data, RBOHB activity could also be supported by the presence of positive
337 regulators such as Rac-like/ROP GTPase. The three Rac-like/ROP GTPase *ARAC1*, *ARAC3* and the
338 homolog of *At4g03100* were induced at 24 hpi. CDPKs such as CPK1 are also known to activate
339 RBOHs in response to increased cytosolic calcium level [61]. But repression of *CPK1* in our data could
340 indicate that this way of activation did not function.

341 In response to abscisic acid (ABA) or microbe-associated molecular pattern (MAMP)
342 immunity, stomatal closure is known to be regulated by apoplastic ROS production (reviewed in [62])
343 and cysteine-rich receptor-like kinases (CRK) are also known to be elements between ROS production
344 and downstream signaling leading to stomatal closure, sometimes activated (CRK10), sometimes

345 inhibited (CRK2 and CRK29; [63]). Three DEGs coding for CRK were found in our data and the
346 repression of *CRK2* and *CRK29* (found two times) could be consistent with the stomata closure
347 previously hypothesized, but the repression of *CRK10* (found two times) was not. Beyond closure,
348 inhibition of stomatal development could be seen as an extreme defense. YODA (found two times)
349 and MPK6 (found two times) MAPKs belong to a pathway involved in the negative regulation of
350 stomata development [64]. These two genes were induced early in our data.

351 To conclude, in pear/*V. inaequalis* nonhost interaction, a calcium influx could lead to the
352 development of the stomatal closure pre-invasive defense, but could also promote a post-invasive
353 defense: apoplastic ROS accumulation. Apoplastic ROS, acting themselves as messengers, could come
354 to strengthen the stomatal closure (Fig. 4).

355

356 Transcription factors and sphingolipids could be implicated in maintaining HR under control in pear /
357 *V. inaequalis* interaction

358 ROS are known to mediate cellular signaling associated with defense-related gene
359 expression, HR i.e. the programmed cell death (PCD) at the site of infection during a pathogen attack,
360 and phytoalexin production [65]. *Arabidopsis thaliana* RCD1 regulator has been proposed to
361 positively regulate cell death in response to apoplastic ROS by protein-protein interactions with
362 transcription factors (reviewed in [66]) and WRKY70 and SGT1b were identified as cell death positive
363 regulators functioning downstream of RCD1 [66]. *RCD1* and *WRKY70* genes were found induced in
364 our data, at 24 hpi and 72 hpi respectively.

365 In *Arabidopsis*, the F-box protein CPR1, in association with the Skp1-Cullin-F-box (SCF)
366 ubiquitin ligase complex, targets for degradation NLR (nucleotide-binding domain and leucine-rich
367 repeats containing proteins) resistance protein such as SNC1, RPM1 or RPS2, to prevent
368 overaccumulation and autoimmunity (reviewed in [67]). A *Skp1-like* (*ASK19*; 72 hpi) gene and *CPR1*
369 (24 hpi) gene were found induced in our data. A gene coding for RPM1 function was also found
370 repressed at 24 hpi. These results could be in favor of the hypothesis that NLR receptors do not take

371 part in the HR development observed in the pear/*V. inaequalis* nonhost interaction (Fig. 1C, H, J). In
372 addition, the induction of an *AtSerpin1* gene homolog at 24 hpi (found two times) in our data could
373 be consistent with that hypothesis. Indeed, AtMC1 is a pro-death caspase-like protein required for
374 full HR mediated by intracellular NB-LRR immune receptor proteins such as RPP4 and RPM1 [68] and
375 AtSerpin1 is a protease inhibitor which block AtMC1 self-processing and inhibit AtMC1-mediated cell
376 death [69].

377 The differential expression of two others components of the proteasome pathway could be
378 in favor of the HR development: the induction of the *RIN3* ubiquitin E3 ligase (24 hpi) and the
379 repression of the *BRG3* ubiquitin E3 ligase (24 hpi). Indeed, RIN3 is known as positive regulator of
380 RPM1 dependent HR [70]. And BRG3 is known as a negative regulator of HR in plant/necrotrophic
381 pathogen interactions [71].

382 Sphingolipids are involved in the control of PCD, either as structural components of
383 membranes but also as initiators in the cell death regulatory pathway. According to Huby et al. [72],
384 free ceramides and long chain/sphingoid base components (LCBs) are able to trigger cell death, via
385 ROS production, whereas their phosphorylated counterparts, ceramide phosphates and long chain
386 base phosphate components (LCB-Ps) promote cell survival. The induction of PCD by LCB is based on
387 the activation of protein kinases, among them MPK6 [73]. As already mentioned, *MPK6* was found
388 early induced in our data and we found numerous DEGs in the nonhost interaction between pear and
389 *V. inaequalis* that seems to indicate the presence of free ceramides and LCB, which could possibly
390 participate to the HR development. Free LCB presence is suggested by the activations of *SBH1* (24
391 hpi), *SLD1* (24 hpi) and another sphingolipid Δ8 long-chain base desaturase homolog to *At2g46210*
392 (24 hpi; found two times), and their relative conversion in ceramides is suggested by the differential
393 expressions of the ceramide synthases *LOH2* (repressed at 24 hpi) and *LOH3/LAG13* (induced at 24
394 and 72 hpi). LCB non-conversion in phosphorylated counterparts could be shown by the *AtLCBK1*
395 repression (72 hpi) and free ceramides maintenance could be suggested by their non-conversion in
396 glycosyled ones given the repression of a glucosyl ceramide synthase homolog to *At2g19880* (24 hpi).

397 The differential expression of numerous known regulators of HR in our data seems again
398 consistent with the HR phenotype observed. The mechanosensor MSL10 and the calmodulin-
399 activated Ca^{2+} pump (autoinhibited Ca^{2+}-ATPase [ACA]) ACA11 were found differentially expressed: at
400 24 hpi *MSL10* was induced and *ACA11* was repressed. MSL10 is known as a positive regulator of cell
401 death [74] and ACA11 is known as a negative regulator of SA-dependent PCD [44]. Their modulation
402 could be linked with the hypothesized calcium influx discussed above [44, 75]. The participation of
403 the SA pathway in the development of the HR could also be supported by the repression of *EDR1* (at
404 72 hpi). Indeed, the MAPKKK EDR1 is known as a negative regulator of the SA-dependent HR
405 (reviewed in [76]).

406 Three other regulators of HR were found modulated in our data. The transcription factor *AS1*
407 (*MYB91*) was found induced at 24 hpi. It is known as a positive regulator of HR and implicated in the
408 JA pathway (reviewed in [31]). The transcription factor *WRKY40* was found repressed at 72 hpi. It is
409 known as a negative regulator of HR [77] and implicated in PTI [78]. Another negative regulator of HR
410 is the lipid-binding domains containing protein VAD1 [79]. It was found repressed at 72 hpi.

411 The behavior of another gene in our data, *UGT73B3,* could indicate that the developed HR
412 was contained due to intracellular ROS production and damages. The function *UGT73B3* was thus
413 activated (24 hpi). UGT73B3 is known as a restrictor of HR expansion via its action in detoxification of
414 ROS-reactive secondary metabolites (UGT73B3; [80]).

415 To conclude, in pear/*V. inaequalis* nonhost interaction, HR was spread out, potentially in link
416 with a calcium influx and ROS production via free sphingolipids accumulation and not via NLR
417 receptors. Furthermore, the behavior of eight regulators seems to indicate that the developed HR is
418 under control (Fig. 4).

419

420 Cell wall carbohydrates content and cuticle composition could be altered in pear / *V. inaequalis*
421 interaction

422 The first obstacle encountered by host as well as nonhost pathogens attempting to colonize
423 plant tissues is the plant cell wall, which is often covered with a cuticle. In nonhost resistance, in
424 which non adapted pathogens normally fail to penetrate nonhost plant cells, the cell wall is
425 considered an important factor and seen as a preinvasive penetration barrier, or as the onset place
426 of defensive signaling pathways [10, 54]. Plant cell wall alterations have been demonstrated to have
427 a significant impact on disease resistance and/or on abiotic stresses. These alterations can concern
428 the carbohydrates or the phenolic components, and results in impairing or overexpressing cell wall-
429 related genes (reviewed in [81] and [82]).

430 We found numerous genes related to the cell wall with a modified expression during nonhost
431 interaction between pear and *V. inaequalis*, among them about thirty related to the biosynthesis or
432 the modification of carbohydrates. These DEGs are presented in Table 4 except those related to the
433 lignin and other phenolic compounds, which will be discussed later. We saw in particular several
434 DEGs related to cellulose (8) and even more DEGs related to pectin (14) but no DEGs related to
435 callose.

436 Concerning these particular carbohydrate components, the model proposed by Bacete et al.
437 [81] is as follows. Firstly, alterations in cellulose biosynthesis from primary or secondary cell wall
438 trigger specific defensive responses, such as those mediated by the hormones JA, ET or abscisic acid
439 (ABA), activate biosynthesis of antimicrobial compounds, but also might attenuate pattern triggered
440 immunity (PTI) responses. Secondly, alterations of cell wall pectins, either in their overall content,
441 their degree of acetylation or methylation, activate specific defensive responses, such as those
442 regulated by JA or SA, and trigger PTI responses, probably mediated by damage-associated molecular
443 patterns like oligogalacturonides. Thus, even though our results do not completely support a role of
444 these DEGs, we suppose that the modified expression of cell wall related genes during nonhost
445 interaction between pear and *V. inaequalis* could be meaningful.

446

447

448 **Table 4: Main DEGs related to cell wall carbohydrates synthesis/modification detected during**

449 **nonhost interaction pear/*V. inaequalis*.**

450

	Gene	Action	Expression*
		Primary cell wall	
Cellulose	*CSLA2*	synthesis	I
	PNT1	synthesis	I
	COBL2	deposition (GPI-anchored protein)	R
	AtGH9A4	catabolism	I
	XTR7	loosening	I
Hemi-cellulose (xyloglucan)	*At5g15490*	synthesis	I
Pectin	*At3g42180*	synthesis	I
	At4g01220	synthesis	I
	GHMP kinase	synthesis	I
	RHM1	synthesis	R
	PME At2g45220	methylesterification	I
	PME At2g46930	methylesterification	I
	PME At3g05910	methylesterification	R
	PME At1g02810	methylesterification	R
	PME44	methylesterification	R
	PG At3g16850	depolymerisation	I
	PG At3g59850	depolymerisation	I
	PG At4g13710	depolymerisation	I
	PG At3g62110	depolymerisation	R
	IDA	degradation	R
Arabinogalactan protein	*AGP11*	_	I
	AGP1	_	R
		Secondary cell wall	
Cellulose	*CESA09*	synthesis	I
	CESA10	synthesis	I
	CSLG1	synthesis	I
Hemi-cellulose (xylan)	*FRA8*	synthesis	I
		Undetermined	
Expansin	*EXP15*	loosening	I
	EXPB3	loosening	I
Hemi-cellulose	*ATFUC1*	modification	I
	XTH33	growth and assembling	R

451 *I: induced, R: repressed
452

453 Concerning the cuticle layer, most cuticles are composed largely of cutin, an insoluble
454 polyester of primarily long-chain hydroxy fatty acids. This lipophilic cutin framework is associated
455 with hydrophobic compounds collectively referred to as waxes. The cuticle is also thought to contain
456 varying amounts of intermingled cell wall polysaccharides and sometimes also a fraction termed
457 cutan (reviewed in [83]). Cutin monomers are synthesized by the modification of plastid-derived 16C
458 and 18C fatty acids in the endoplasmic reticulum (ER), yielding variously oxygenated fatty acid–
459 glycerol esters referred to as monoacylglycerols, which polymerize upon arrival at the growing cuticle
460 (Fig. 5, reviewed in [83]).

461 C16 and C18 fatty acids are also important precursors of cuticular wax synthesis (Fig. 5).
462 Upon transport to the ER, the C16 and C18 fatty acids are extended to form very-long-chain fatty
463 acids (VCLFAs; C>20), and this extension is carried out by the fatty acid elongase (FAE) complex
464 located on the ER membrane. The very-long-chain FAs are then converted into the varied cuticular
465 waxes (primary alcohols, aldehydes, alkanes, secondary alcohols, ketones) by many ways (reviewed
466 in [84]).

467 Interestingly, we found three genes up-regulated 24 hpi belonging to the FAS (fatty acid
468 synthase) chloroplastic complex implicated in the production of the C16 precursor (Fig. 5): *ACCD*,
469 *FabG* and *MOD1* (found two times). ACCD encodes the carboxytransferase beta subunit of the
470 Acetyl-CoA carboxylase complex which catalyzes the first committed step in fatty acid synthesis: the
471 carboxylation of acetyl-CoA to produce malonyl-CoA. FabG and MOD1 are respectively a β-ketoacyl
472 ACP-reductase and an enoyl-ACP-reductase which catalyze respectively the conversion of
473 acetoacetyl-ACP into β-hydroxyacyl-ACP and the second reductive step from enoyl-ACP to butyryl-
474 ACP (reviewed in [84]).

475 In the ER, the four functions we found related to waxes biosynthesis in our data were
476 repressed at 24 hpi: *KCS4* (found two times), *CER1* and *CER3*, or 72 hpi: *ECR/CER10*. KCS4 and
477 ECR/CER10 belong to the FAE complex ([85]; [86]). The last two genes are implicated in aldehydes

478 (*CER1*) and alkanes (*CER1 and 3*) generation (reviewed in [84]). On the contrary, the eight genes we
479 found related to cutin biosynthesis were induced at 24 hpi except a gene homolog to *At5g14450*,
480 which was induced at 72 hpi. One of them is a glycerol-3-phosphate acyltransferase (GPAT) coding
481 gene: GPAT8, which catalyzes the transfer of a fatty acid from coenzyme A (CoA) to glycerol-3-
482 phosphate (Fig. 4; reviewed in [83]). GPAT8 function in cutin formation has been functionally
483 confirmed in association with GPAT4 [87]. The seven others genes code GDSL-lipases enzyme
484 (*At1g28600*, *At1g28660*, *At1g54790*, *At3g16370*, *At3g48460*, *AtCUS4*: *At4g28780*, *At5g14450*), some
485 of which have been shown to function as cutin synthase (Fig. 4; [88]; reviewed in [83]) and
486 polymerize monoacylglycerols.

487 We also found induced respectively at 24 and 72 hpi two genes involved in waxes and cutin
488 biosynthesis positive regulation: *MYB16* and *SHN1*. The SHN genes (*SHN1–SHN3*), a set of three
489 largely redundant APETALA 2 family transcription factors from *A. thaliana*, are regulators of floral
490 cutin and epidermal cell morphology. SHN1 is regulated by the MYB family transcription factor
491 MYB106, which, along with its paralog MYB16, controls many aspects of cuticle and epidermis
492 formation in *A. thaliana* (reviewed in [89] and [83]).

493 Cutin and cuticular waxes play an important role in plant-insect and plant-microbe
494 interactions. Numerous *Arabidopsis* mutants in cutin and waxes biosynthetic or transport genes, such
495 as Acyl-CoA binding proteins (ACBP), show varying degrees of cuticle impairment, alterations in cutin
496 and/or wax composition, and defects in SAR (reviewed in [84]). We found *ACBP6* repressed at 24 hpi.
497 That repression is not inconsistent with the previously described possible amplification of cutin
498 biosynthesis and polymerization, given that *acbp6* KO mutation is not associated with a defect in that
499 pathway [50]. That repression is also consistent with the SAR repression hypothesized above as the
500 *acbp6* KO mutant show compromised SAR [50].

501 To conclude, our analysis of nonhost pear/V. *inaequalis* interaction could show an alteration
502 of the cuticle composition with more cutin and less waxes synthesis. The potential increase in cutin

503 polymerization could lead to a thickening of the cuticular layer to prevent fungus penetration via its
504 appressoria.
505
506 Secondary metabolism seems to lead to G unit lignin polymerization and simple coumarin or
507 hydroxycinnamic acid amine phytoalexins synthesis in pear / *V. inaequalis* interaction
508 As distinguished from primary metabolism, plant secondary metabolism refers to pathways
509 and small molecule products of metabolism that are non-essential for the survival of the organism.
510 But they are key components for plants to interact with the environment in the adaptation to both
511 biotic and abiotic stress conditions. Plant secondary metabolites are usually classified according to
512 their chemical structure. Several groups of large molecules, including phenolic acids and flavonoids,
513 terpenoids and steroids, and alkaloids have been implicated in the activation and reinforcement of
514 defense mechanisms in plants (reviewed in [90]).
515 Terpenoids and steroids, or isoprenoids, are components of both the primary and secondary
516 metabolisms in cells, and mono-, tri-, sesqui- and polyterpenes are considered as secondary
517 metabolites (reviewed in [91]). Our results on pear identified seven DEGs and five DEGs which could
518 belong to the chloroplastic methylerythritol posphate (MEP) and to the cytosolic mevalonic acid
519 (MVA) pathway of isoprenoids production respectively (Table 5), which results, among others
520 compounds, in tri- and sesquiterpenes secondary metabolites. The majority of these genes
521 contribute to produce primary metabolites according to Tetali [91]. Except *SMT2*, that we found
522 induced at 24 hpi, there is no report concerning a putative implication of others genes in plant biotic
523 resistance. SMT2 is involved in sterols production and *smt2* mutation was reported to compromise
524 bacterial resistance in *Nicotiana benthamiana* [92]. The hypothesis is that sterols regulate plant
525 innate immunity against bacterial host and nonhost infections by regulating nutrient efflux into the
526 apoplast. *V. inaequalis* is a hemibiotrophic pathogen which colonizes only the apoplast compartment
527 at the beginning of the interaction. Strong relative induction of *SMT2* in our data could indicate that a

528 similar mechanism of nutrient efflux regulation via sterols could take place to limit the fungus growth

529 in pear nonhost resistance against *V. inaequalis*.

530

531

532 **Table 5: Main DEGs involved in biosynthetic pathways for terpenes and isoprenoids during pear/*V.***

533 ***inaequalis* nonhost interaction.**

	Gene	Function	Expression*
Cytosolic MVA (mevalonic acid) pathway enzymes	*HMGS*	catalyze the second step of the pathway	R
	HMGR1	catalyze the third step of the pathway	R
	SMT2	sterols production	I
	FLDH	sesquiterpenes production	R
	SQE2	triterpenes production	I
Chloroplastic MEP (methylerythritol posphate) pathway enzymes	*DXR*	catalyzes the second step of the pathway	I
	GG reductase	chlorophylls production	R
	VTE4	tochopherols production	I
	KAO1	gibberellins production	R
	PDS2	plastoquinones production	I
	LYC	carotenoids production	I
	PGGT1	covalent attachment of a prenyl group to a protein	I

534 *I: induced, R: repressed

535

536 In our data, the other DEGs that were linked to secondary metabolism belong to the

537 phenylpropanoid pathway production (Fig. 6). Among them we found four genes which could belong

538 to the flavonoid production, all repressed, at 24 hpi (*DFR* and *DRM6*) or 72 hpi (*TT7* and *UGT71D1*).

539 DFR (dihydroflavonol reductase) is involved in flavan-3,4-ol production and TT7 (flavonoid 3'

540 hydroxylase) in dihydroquercetin production from dihydro-kaempferol, and UGT71D1 (glucosyl

541 transferase) in quercetin-glycoside production from quercetin (TAIR database;

542 https://www.arabidopsis.org/index.jsp). DMR6 (flavone synthase) is involved in flavone production

543 from naringenin [93]. Thus flavonoid production does not seem to be favored, which is not consistent

544 with the induction of *MYB12* at 24 hpi, but consistent with *MYB4* induction at 72 hpi. MYB12 is

545 actually known as a positive regulator of flavonol biosynthesis in pear and apple fruits [94, 95]

546 whereas MYB4 is known as a negative regulator of this biosynthetic pathway [96].

547 Concerning the production of monolignols, precursors of lignin synthesis, some genes
548 potentially related were found induced, others repressed. We found *CYP98A3* and *CAD9* (found two
549 times) induced at 24 hpi and *HCT*, *CCR1* and a gene homolog to *At2g23910* (found two times, one
550 time repressed at 24 hpi, one time repressed at 72 hpi, Fig. 6). *CYP98A3* encodes a C3H (coumarate
551 3-hydroxylase), *CAD9* encodes a CAD (cinnamyl alcohol dehydrogenase), HCT is an
552 hydroxycinnamoyl-CoA shikimate/quinate hydroxycinnamoyl transferase, *CCR1* encodes a CCR
553 (cinnamoyl-CoA reductase) and *At2g23910* encodes a CCR-related protein. (TAIR and KEGG
554 databases (https://www.genome.jp/kegg/)).
555 Lignification is obtained by cross-linking reactions of the lignin monomers or by polymer–
556 polymer coupling via radicals produced by oxidases such as peroxidases [97] and laccases [98].
557 However, while peroxidases are able to oxidize monolignols to produce H, G and S units of lignin,
558 laccases only generate G units [97]. In our data, we found two laccases induced at 24 hpi: *LAC11*
559 (found two times, one time induced at 24 and 72 hpi) and *LAC17* (found two times), and three
560 peroxidases repressed at 24 hpi: *PRX17*, *PER47* and *PRX52* (also repressed at 72 hpi), which could be
561 linked to lignin biosynthetic process (Fig. 6). According to Zhao et al. [98], LAC11 and LAC17, along
562 with LAC4, play a critical role in lignification, and their results suggests that peroxidase and laccase do
563 not serve redundant functions in lignification, at least in the vascular tissues of the stem and root of
564 *Arabidopsis*. Participation in lignin formation has also been proved for PRX17 [99], PER47 [100] and
565 PRX52 [101]. But there are currently no reports about a possible involvement of all these genes in
566 lignification linked to biotic or abiotic stresses. Concerning nonhost resistance, two reports describe
567 lignin accumulation/deposition involvement: one in apple fruit [102] and the other one in cowpea
568 [103]. In the latest, authors showed that preferentially generated lignin units in this nonhost
569 interaction are G units, just as it could be the case in our pear / *V. inaequalis* study. To summarize, it
570 is tempting to think that modifications of expression observed for genes linked to lignin
571 polymerization are relevant for the pear nonhost resistance against *V. inaequalis*, but further
572 functional analysis should be conducted to conclude about the lignin status, such as histochemical

573 staining [104], content measure by absorbance [104] or Fourier-transform infrared (FTIR)
574 spectroscopy analysis [105].

575 The biosynthesis of two others types of phenylpropanoid compounds could appear to be
576 favored during pear nonhost resistance against *V. inaequalis*: simple coumarin on one hand and
577 hydroxycinnamic acid amides on the other hand. We found four *BGLU*-like genes induced: *BGLU47*
578 and *BGLC3* (at 24 hpi), *BGLU16* (at 72 hpi); *BGLU42* (at 24 and 72 hpi) (Fig. 6). These β-glucosidases
579 could be implied in simple coumarin path production from the cinnamic acid (KEGG database). Some
580 natural simple coumarins are known as antifungal compounds *in vitro* and have been developed as
581 fungicides [106]. Previous work on Hevea also reports the correlation between the resistance against
582 pathogenic fungi and the production of some coumarins, with antifungal activity *in vitro* [107]. We
583 also found induced at 24 hpi the genes *AACT1/ACT1*, *ATPAO5* and genes homologs to *At4g17830* and
584 *At4g38220* (Fig. 6). AACT1/ACT1 catalyze the first specific step in branch pathway synthesizing
585 hydroxycinnamic acid amides from the p-Coumaroyl CoA or the feruloyl CoA and amines agmatine or
586 putrescine [108]. Hydroxycinnamic acid amides are produced in response to pathogenic infections
587 [108] and surface exported. Hydroxycinnamic acid amides are reported to participate in *Arabidopsis*
588 nonhost resistance against *Phytophthora infestans* via their inhibitory activity on spore germination
589 [109]. The three others genes belong to the arginine biosynthesis path (homologs to *At4g1783* and
590 *At4g38220*) and the arginine and proline metabolisms which produce the amines agmatine and
591 putrescine (*ATPAO5*) (KEGG database). Agmatine is directly produced from arginine thanks to an ADC
592 activity (arginine decarboxylase) and putrescine can be produced from spermidine thanks to a PAO
593 activity (polyamine oxidase). ATPAO5 catalyzes the conversion of spermine in spermidine. The
594 induction of these three last genes is therefore consistent with the hypothesis of amines production
595 in order to enable hydroxycinnamic acid amides synthesis. The induction of *C4H* at 24 hpi could also
596 favor hydroxycinnamic acid amides synthesis via p-Coumaroyl CoA biosynthesis promotion. C4H
597 (cinnamate 4-hydroxylase) catalyzes the production of p-Coumaric acid from Cinnamic acid and p-
598 Coumaric acid gives p-Coumaroyl CoA thanks to 4CL (4- coumarate-CoA ligase) (KEGG database).

599 Among the suite of defense components synthetized in nonhost as in host context, a
600 chemical barrier can be established via accumulation of a diverse array of secondary metabolites
601 rapidly produced upon pathogen infection, named phytoalexins, with toxic or inhibitory effects
602 (reviewed in [10]). Phytoalexins can be flavonoids, such as the pisatin of pea (in [110]) but also varied
603 phenylpropanoid compounds. In the nonhost interaction pear / *V. inaequalis*, the production of
604 flavonoid type phytoalexins does not seem to be favored, except possibly simple coumarin and
605 hydroxicinnamic acid amines.
606
607 Very limited transcriptomic modulation during apple / *V. pyrina* nonhost interaction
608 Only 60 DEGs were detected in the apple / *V. pyrina* nonhost interaction at 24 or 72 hpi, in
609 agreement with the total absence of macroscopic symptoms and few cells engaged in an HR-like
610 reaction observed at the microscopic level. Among these 60 DEGs, 36 have unpredicted function.
611 Among the 24 remaining DEGs, nine DEGS could be relevant in apple / *V. pyrina* nonhost interaction
612 in view of our findings in pear / *V. inaequalis* nonhost interaction. *ORG2* (*BHLH038*), a putative
613 integrator of various stress reactions [111] was induced at 24 hpi. Three genes were related to an
614 oxidative stress: *GASA10* was repressed at 24 hpi and *NRAMP3* and *AOR* were induced at 24 hpi.
615 GASA proteins have been suggested to regulate redox homeostasis via restricting the levels of $OH^{\cdot}$ in
616 the cell wall [112]. The repression of this gene could be thus in favor of more $OH^{\cdot}$ in the cell wall. The
617 oxidoreductase coding gene *AOR* is known in the chloroplast to contribute to the detoxification of
618 reactive carbonyls produced under oxidative stress [113]. *NRAMP* genes function as positive
619 regulators of ROS accumulation, especially during *Arabidopsis Erwinia chrisanthemi* resistance [114].
620 The induction (at 24 and 72 hpi) of another gene could suggest modifications at the cell wall level:
621 *EXP8*, an expansin coding gene involved in cell wall loosening (Tair database). We also found two
622 genes related to hormone pathways, one induced at 24 hpi: *WIN1* and the other one repressed at 72
623 hpi: *UBP12*. WIN1 is known as a negative regulator of SA pathway [115] and UBP12 as a positive
624 regulator of JA pathway via the stabilization of MYC2 [29]. In possible link with the JA pathway, we

625 also found *TPS21* induced at 24 hpi. TPS21 is involved in sesquiterpenes production and is promoted
626 by JA signal via MYC2 [116]. TPS21 is especially involved in the jasmonate-dependent defensive
627 emission of herbivore-induced volatiles in cranberries [117]. Finaly the last DEG we found potentially
628 relevant in apple / *V. pyrina* nonhost interaction could promote HR via ceramides accumulation.
629 *ACD11* is repressed at 24 hpi in our data. In *acd11* mutants, the relatively abundant cell death
630 inducer phytoceramide rises acutely [118].

631 Because nonhost resistance of apple against *V. pyrina* has resulted in a very limited number
632 of cells engaged in an HR-like reaction, it has not been possible for us to exhaustively describe its
633 outcome at the transcriptomic level in the first three days of the interaction. Further insight with
634 later points of kinetic and more adapted techniques such as laser-assisted cell picking, prior to micro
635 arrays or RNA sequencing analysis (review in [119]) could provide more information in the future.

636

637 Comparison of pear resistances against the host pathogen *V. pyrina* and the nonhost pathogen *V.*
638 *inaequalis*

639 Perchepied et al. [13] performed a detailed transcriptomic analysis of the host resistance of
640 pear against *V. pyrina* strain VP102, deployed in a transgenic pear bearing the well-known apple *Rvi6*
641 resistance gene against *V. inaequalis*. Comparing this work to ours gives us the rare opportunity to
642 analyze similarities and differences between a host and a nonhost resistance in the same plant.

643 Concerning the recognition and early signaling steps of the interactions, many receptors and
644 co-receptors have been found induced in the host pear resistance, especially damage-associated
645 molecular patterns receptors such as RLK7, revealing that PTI and ETI must be engaged. We did not
646 find evidence of the mobilization of such receptors in the pear nonhost resistance. PTI and ETI
647 receptors are nonetheless reported as implicated in nonhost resistance (reviewed in [120] and [10]).
648 As we only analyzed post infection transcriptional modulations in the nonhost pear/*V. inaequalis*
649 interaction (at 24 and 72 hpi), one hypothesis to explain the lack of PTI and ETI receptors in our data
650 could be that these receptors were already present as preformed defenses and not particularly

651 induced by the infection onset. In pear nonhost interaction, the earliest likely signaling pathways we
652 were able to highlight are calcium influx and apoplastic ROS production. Calcium signaling seems to
653 be also implicated in pear host resistance, but less obviously than it seems in nonhost resistance.

654 Regarding the hormonal signaling pathways, the JA defense signaling pathway seems to be
655 repressed in pear nonhost resistance but was found quite activated in pear host resistance. The
656 JA/ethylene (ET) defense signaling pathway is known as an effective defense against necrotrophic
657 fungi in *Arabidopsis* [121]. Thus, it is not inconsistent to find the JA pathway potentially repressed in
658 the development of the pear nonhost resistance against the hemi-biotrophic pathogen *V. inaequalis*.
659 But it is very interesting to find this pathway rather induced in the development of the pear host
660 resistance against the other hemi-biotrophic pathogen *V. pyrina*. The SA signaling pathway is
661 commonly seen as the classical one triggered to resist biotrophic fungi in *Arabidopsis* [121], but it
662 seems only a little engaged in pear nonhost resistance , and is repressed in pear host resistance. If
663 this absence of SA implication is quite unexpected in pear host resistance against a hemi-biotrophic
664 fungus, it could be consistent with the report that the exact role of these key defense
665 phytohormones is unclear in nonhost resistance and remains to be established [54]. As shown by
666 Tsuda et al. [122], an explanation for the hormone pathways behavior in pear host resistance could
667 be that: as both the SA and JA/ET pathways positively contribute to immunity, a loss of signaling flow
668 through the SA pathway can be compensated by a rerouting signal through the JA/ET pathways. In
669 addition, independently of SA signaling, but in positive connection with JA signaling, SAR seems to be
670 engaged in distal tissues during pear host resistance. To conclude, in pear host as well as nonhost
671 resistances, classical resistance hormones SA and JA/ET, and the correlative PR gene defenses, seems
672 differently involved than in *Arabidopsis*.

673 The carbohydrate content of the cell-wall seems to be modified in response to the attacks by
674 the pathogens. Regarding cell-wall and cuticle, in pear host as well as nonhost resistances, the
675 numerous DEGs found could highlight important modifications. Similar modifications affected the
676 cellulose and mainly the pectin contents, but no callose production was observed. Regarding cuticle,

677 waxes production was induced in host resistance whereas it seems to be repressed in nonhost
678 resistance, in favor of cutin production / polymerization, which was also induced in host resistance.
679 To conclude, as a first obstacle encountered by host, as well as nonhost pathogens attempting to
680 colonize plant tissues, the plant cell wall and its cuticle seem to play a leading role in both pear host
681 and nonhost resistances.

682 Finally, the production of secondary metabolites and phenylpropanoids compounds in
683 particular, could be a major line of defense, in pear host as well as nonhost resistances, but with
684 divergences. If lignin and flavonoid productions are preponderant in pear host resistance against *V.*
685 *pyrina*, lignin implication in pear nonhost resistance seems less clear and flavonoids production
686 seems repressed. But the biosynthesis of two other types of phenylpropanoid-derived phytoalexins
687 could be favored during pear nonhost resistance: simple coumarin on one hand and hydroxycinnamic
688 acid amides on the other hand.

689 The comparative analysis between a host and a nonhost resistance in pear shows that, even
690 though specificities are observed, two major defense lines engaged seems shared: the cell wall and
691 its cuticle on one hand, the secondary metabolism with the phenylpropanoid pathway on the other
692 hand. Moreover, these defenses seem deployed independently of the SA signaling pathway, yet
693 widely recognized as the main defense hormone against biotrophic pathogens.

694

695 Conclusion

696 To our knowledge, our work is the first one published regarding a transcriptomic analysis of
697 post-infections events of a nonhost resistance to *Venturia sp.* in apple and pear. Here, our molecular
698 work on apple / *V. pyrina* nonhost resistance remains preliminary and in order to allow a deeper
699 deciphering, further analyses must be considered with the aid of tools adapted to this nonhost
700 resistance with very few cells engaged in an HR-like reaction, only visible at a microscopic level. In
701 pear, this deciphering allowed us to show that nonhost resistance against *V. inaequalis* involves

702 enough pathogen penetration in plant tissue to occasionally trigger visible HR, and develops post-
703 invasive defenses.

704 To summarize our findings on pear with a notion of cascading effect, we can propose the
705 following scenario (Fig. 4): once *V. inaequalis* presence is recognized by pear, a calcium cellular influx
706 could be induced and could lead to the possible development of a pre-invasive defense, the stomatal
707 closure, but could also promote a possible early post-invasive defense, an apoplastic ROS
708 accumulation. Apoplastic ROS, acting themselves as ubiquitous messengers, could come to reinforce
709 the stomatal closure but could also mediate cellular signaling possibly resulting in two post-invasive
710 defenses: HR development at infection sites, along with phytoalexin (simple coumarin and
711 hydroxicinnamic acid amines) production. The inferred alterations of the epidermis composition
712 (cellulose, pectin, lignin for the cell wall, and cutin for the cuticle), are presumed to strengthen this
713 physical barrier and could be seen as the development of another pre-invasive defense. Nonhost
714 resistance is defined as the resistance of an entire plant species against a specific parasite or
715 pathogen and is seen as the most durable resistance of plant. Thus, understanding the molecular
716 mechanisms underlying nonhost resistance can open up some interesting avenues to create
717 sustainable host resistances in the same plant species. Considering pear, in order to stop the
718 germination and entrance of hemibiotrophic host fungi such as *V. pyrina*, strengthening the cuticle
719 initial barrier via more cutin production and cross-link, or promoting the biosynthesis of phytoalexins
720 like hydroxycinnamic acid amines, appear as promising solutions.

721

722 **Material and methods**

723 Biological material

724 Apple plants from the cultivar 'Gala' and pear plants from the cultivar 'Conference' were
725 chosen because of their susceptibility to *V. inaequalis* and *V. pyrina*, respectively. The apple and pear
726 genotypes were multiplied *in vitro*, rooted and acclimatized in greenhouse as described previously
727 [123, 124].

728 For apple scab inoculation, the *V. inaequalis* monoconidial isolate used was EU-B05 from the
729 European collection of *V. inaequalis* of the European project Durable Apple Resistance in Europe
730 [125]. For pear scab inoculation, the monoconidial strain VP102 of *V. pyrina* was chosen for its
731 aggressiveness on 'Conference' [126].
732
733 Scab inoculation procedure
734 Greenhouse growth conditions and mode of inoculum preparation were as described in Parisi
735 and Lespinasse [127] for apple and Chevalier et al. [128] for pear. Briefly, the youngest leaf of actively
736 growing shoots was tagged and the plants inoculated with a conidial suspension (2×10^5 conidia ml^{-1})
737 of *Venturia pyrina* strain VP102 for apple and *Venturia inaequalis* strain EUB04 for pear. Symptoms
738 were recorded at 14, 21, 28, 35 and 42 days after inoculation on 20 actively growing shoots (one
739 shoot by plant) for each interaction. The type of symptoms was scored using the 6 class-scale of
740 Chevalier et al. [129].
741
742 Microscopic observations
743 Histological studies were made on samples stained with the fluorophore solophenylflavine
744 [130]. In brief, leaf discs were rinsed in ethanol 50° before staining in a water solution of
745 solophenylflavine 7GFE 500 (SIGMA-Aldrich, St Louis USA) 0.1% (v/v) for 10 min. The samples were
746 first rinsed in deionized water, then in 25% glycerol for 10 min. Finally, the leaf samples were
747 mounted on glass-slides in a few drops of 50% glycerol. They were examined with a wide-field
748 epifluorescence microscope BH2-RFC Olympus (Hamburg, D) equipped with the following filter
749 combination: excitation filter 395 nm and emission filter 504 nm.
750
751 Transcriptomics experiment
752 Leaf samples were immediately frozen in liquid nitrogen and kept at -80°C until analysis.
753 Sampling concerned the youngest expanded leaf of each plant labeled the day of the inoculation.
754 Each biological repeat is a pool of three leaves from three different plants and two biological repeats

755 (n=2) have been made by condition (genotype x treatment x time). Leaf samples taken just before
756 inoculation (T0) and at 24 and 72 hpi, were then used to perform transcriptomics analyses.

757 For RNA extraction, frozen leaves were ground to a fine powder in a ball mill (MM301,
758 Retsch, Hann, Germany). RNA was extracted with the kit NucleoSpin RNA Plant (Macherey Nagel,
759 Düren, Germany) according to the manufacturer's instructions but with a modification: 4% of PVP40
760 (4 g for 100 ml) were mixed with the initial lysis buffer RAP before use. Purity and concentration of
761 the samples were assayed with a Nanodrop spectrophotometer ND-1000 (ThermoFisher Scientific,
762 Waltham, MA, USA) and by visualization on agarose gel (1% (weight/volume) agarose, TAE 0.5x, 3%
763 (volume/volume) Midori green). Intron-spanning primers (forward primer:
764 CTCTTGGTGTCAGGCAAATG, reverse primer: TCAAGGTTGGTGGACCTCTC) designed on the *EF-1α* gene
765 (accession AJ223969 for apple and PCP017051 for pear, available at https://www.rosaceae.org/, with
766 the datasets on "*Pyrus communis* v1.0 draft genome") were used to check the absence of genomic
767 DNA contamination by PCR. The PCR reaction conditions were as follows: 95°C for 5 min, followed by
768 35 cycles at 95°C for 30 s, 60°C for 45 s, 72°C for 1 min, with a final extension at 72°C for 5 min. The
769 PCR products were separated on a 2% agarose gel.

770 Amplifications (aRNAs) were produced with MessageAmpII aRNA Kit (Ambion Invitrogen,
771 Waltham, MA, USA), from 300 ng total RNA. Then 5 µg of each aRNA were retrotranscribed and
772 labelled using a SuperScript II reverse transcriptase (Transcriptase inverse SuperScript™ II kit,
773 Invitrogen, Carlsbad, CA, USA) and fluorescent dyes: either cyanine-3 (Cy3) or cyanine-5 (Cy5)
774 (Interchim, Montluçon, France). Labeled samples (30 pmol each, one with Cy3, the other with Cy5)
775 were combined two by two, depending on the experimental design (i. e. for example, the
776 CF/EUB05/24 hpi sample and the CF/non inoculated sample are labeled with Cy3 and Cy5
777 respectively and pooled to co-hybridize the microarray) . For each comparison two biological
778 replicates were analyzed in dye-switch as described in Depuydt et al. [131]. Paired labeled samples
779 were then co-hybridized to Agilent microarray AryANE v2.0 (Agilent-070158_IRHS_AryANE-Venise,
780 GPL26767 at GEO: https://www.ncbi.nlm.nih.gov/geo/) for apple, or Pyrus v1.0 (Agilent-

781 078635_IRHS_Pyrus, GPL26768 at GEO) for pear, containing respectively 133584 (66792 sense and
782 66792 anti-sense probes) and 87812 (43906 sense and 43906 anti-sense probes) 60-mer
783 oligonucleotide probes. The hybridizations were performed as described in Celton, Gaillard et al.
784 [132] using a MS 200 microarray scanner (NimbleGen Roche, Madison, WI, USA).

785 For microarray analysis we designed two new chips. For apple we used a deduplicated
786 probeset from the AryANE v1.0 ([132]; 118740 probes with 59370 in sense and 59370 in anti-sense)
787 augmented by 14844 probes (7422 in sense and 7422 in anti-sense) designed on new gene
788 annotations from *Malus x domestica* GDDH13 v1.1 (https://iris.angers.inra.fr/gddh13 or
789 https://www.rosaceae.org/species/malus/malus_x_domestica/genome_GDDH13_v1.1). These
790 probes target new coding genes with UTRs when available, manually curated micro-RNA precursors
791 and transposable elements. For transposable elements we used one consensus sequence for each
792 family and a randomly peaked number of elements proportional to their respective abundance in the
793 genome. The microarrays used in this study also have probes for coding genes of *V. inaequalis* but
794 they have not been taken into account.

795 For pear the design was done on the *Pyrus communis* Genome v1.0 Draft Assembly &
796 Annotation available on GDR
797 (https://www.rosaceae.org/species/pyrus/pyrus_communis/genome_v1.0) web site. We have
798 downloaded the reference genome and gene predictions fasta files and structural annotation gff file
799 the 21st of September 2015. Using home-made Biopython scripts we have extracted spliced CDS
800 sequences with 60 nucleotides before start and after stop codons to get UTR-like sequences likely to
801 be found on transcripts resulting in a fasta file containing 44491 sequences. These 60 nucleotides
802 increase the probability of finding specific probes on genes with high similarity. This file was sent to
803 the eArray Agilent probe design tool (https://earray.chem.agilent.com/earray/) to generate one
804 probe per gene prediction. Options used were: Probe Length: 60, Probe per Target: 1, Probe
805 Orientation: Sense, Design Options: Best Probe Methodology, Design with 3' Bias. The probeset was
806 then reverse-complemented to generate anti-sense probes and filtered to remove duplicated

807 probes. The final probeset contains 87812 unique probes targeting 1 (73612 probes) or more (14200
808 probes) potential transcript both in sense and anti-sense.
809 Normalization and statistical analyses performed to get normalized intensity values have
810 been done as in Celton, Gaillard et al. [132]. Briefly, data were normalized with the lowess method,
811 and differential expression analyses were performed using the lmFit function and the Bayes
812 moderated t-test with the LIMMA package in R software [133, 134]. The pipeline AnaDiff used for
813 these differential analyses is available at https://zenodo.org/record/6477918#.Yn5O3XVBzIE [135].
814 For each comparison and each probe, we retrieved a ratio of the logarithms of the fluorescence
815 intensities (one per compared sample: T0 versus 24 hpi or T0 versus 72 hpi in our case) and an
816 associated p-value. The applied p-value threshold to determine DEGs (differentially expressed genes)
817 was 0.01. Through blast analysis, a TAIR accession number (The *Arabidopsis* Information Resource;
818 https://www.arabidopsis.org/; [136]) has been linked to a majority of apple or pear
819 "probe/corresponding gene". Thanks to the Functional Classification SuperViewer tool [137], the
820 TAIR accessions have then been used to class DEGs in functional categories according to MapMan
821 software (https://mapman.gabipd.org/homemapman.gabipd.org; file
822 Ath_AGI_LOCUS_TAIR10_Aug2012.txt; [138]), and to highlight the enriched ones by calculating the
823 frequency of DEGs per category, normalized to the numbers of *Arabidopsis* genes in each MapMan
824 category, and bootstrapping the dataset to provide a confidence estimate for the accuracy of the
825 result. The detailed analysis of DEGs has been done through TAIR and KEGG
826 (https://www.genome.jp/kegg/) databases, and bibliography. Metadata for the 193 (184 for pear,
827 corresponding to 158 different functions and 9 for apple) DEGs discussed in this work are available in
828 Table S2 and S4 (Online only).
829
830 qPCR validation of transcriptomic data
831 In order to validate transcriptomic data, qPCR was performed on a selection of gene/sample
832 associations. First-strand cDNA was synthesized using total RNA (2.0 µg) in a volume of 30 µl of 5×

833 buffer, 0.5 µg of oligodT15 primer, 5 µl of dNTPs (2.5 mM each), and 150 units of MMLV RTase
834 (Promega, Madison, WI, USA). The mixture was incubated at 42°C for 75 min. qPCR was then
835 performed. Briefly, 2.5 µl of the appropriately diluted samples (1/16 dilution) were mixed with 5 µl of
836 PerfeCTa SYBR Green SuperMix for iQ kit (Quantabio, Beverly, MA, USA) and 0.2 or 0.6 µl of each
837 primer (10 µM) in a final volume of 10 µl. Primers were designed with Primer3Plus, their volumes
838 were according to their optimal concentration (determined for reaction efficiency near to 100%;
839 calculated as the slope of a standard dilution curve; [139]). Accessions, primer sequences and
840 optimal concentrations are indicated in Table S1. The reaction was performed on a CFX Connect Real-
841 Time System (BIO-RAD, Hercules, CA, USA) using the following program: 95°C, 5 min followed by 40
842 cycles comprising 95°C for 3 s, 60°C for 1 min. Melting curves were performed at the end of each run
843 to check the absence of primer-dimers and nonspecific amplification products. Expression levels
844 were calculated using the ΔΔCT method [140] and were corrected as recommended in
845 Vandesompele et al. [141], with three internal reference genes (GADPH, TUA and ACTIN 7 for apple,
846 GADPH, TUA and EF1α for pear) used for the calculation of a normalization factor. For each couple
847 DEG/sample (sample defining a plant, time, treatment and biological repeat combination), the ratio
848 was obtained by dividing the mean value of CT calculated from 3 technical repeats by the
849 normalization factor obtained for this sample.
850

851 ## Supplementary information

852 **Additional File 1: Table S1**, **S2, S3, S4 and S5**.
853

854 ## Abbreviations

855 ABA: abscisic acid; CDPK: calcium dependent protein kinase; CRK: cysteine-rich receptor-like kinase;
856 DEG: differentially expressed gene; DFR: dihydroflavonol 4-reductase; DGDG:
857 digalactosyldiacylglycerol; ET: ethylene; ER: endoplasmic reticulum; ETI: effector triggered immunity;
858 FAE: fatty acid elongase; GPAT: glycerol-3-phosphate acyltransferase; hpi: hours post inoculation; HR:

859 hypersensitive reaction; JA; jasmonic acid; LCB: long chain/sphingoid base component; LCB-Ps: long
860 chain base phosphate component; LOX: lipoxygenase; MAMP: microbe-associated molecular pattern;
861 OPDA: 12-oxo-phytodienoic acid; PCD: programed cell death; PTI: pattern triggered immunity; RBOH:
862 respiratory burst oxidase homolog; ROS: reactive oxygen species; SA: salicylic acid; SAR: systemic
863 acquired resistance
864

865 **Declarations**

866 Acknowledgements
867 The authors gratefully acknowledge the IRHS-ImHorPhen team of INRA Angers for technical
868 assistance in plant maintenance and the technical platforms ANAN and IMAC.
869 Authors contribution
870 EC, LP, and EV conceived the study. EC and EV supervised the study. ER and MB performed the
871 biological experiments. SG and SP performed the database work and assisted with the bioinformatics
872 analysis. EV wrote the original manuscript. EV and EC edited the manuscript. All authors have read
873 and agreed to the published version of the manuscript.
874 Funding
875 This project was funded by the Synthé-Poir-Pom project (Angers University) and by the TIFON project
876 (INRAE, department BAP).
877 Availability of data and materials
878 The datasets supporting the conclusion of this article are available in the Gene Expression Omnibus
879 (GEO) repository [https://www.ncbi.nlm.nih.gov/geo/] with GSE159179 and GSE159180 accession
880 numbers for apple and pear respectively [142, 143]. The pipeline AnaDiff used for differential
881 analyses is available at https://zenodo.org/record/6477918#.Yn5O3XVBzIE [135].
882 Ethics approval and consent to participate
883 Experimental research on plants in this work comply with relevant institutional, national, and
884 international guidelines and legislation.

885 Consent for publication

886 This section is not applicable.

887 Competing interests

888 The authors declare that they have no competing interests.

889

890 ## References

891 1. Potter D, Eriksson T, Evans RC, Oh S, Smedmark JEE, Morgan DR, Kerr M, Robertson KR, et al.
892 Phylogeny and classification of *Rosaceae*. Plant Syst Evol. 2007;266:5-43.

893 2. Campbell CS, Evans RC, Morgan DR, Dickinson TA, Arsenault MP. Phylogeny of subtribe *Pyrinae*
894 (formerly the *Maloideae*, *Rosaceae*): Limited resolution of a complex evolutionary history.
895 Plant Syst Evol. 2007;266: 119-145.

896 3. Wu J, Wang Z, Shi Z, Zhang S, Ming R, Zhu SL et al. The genome of pear (*Pyrus bretschneideri*
897 Redh.). Genome Res. 2013;23:396-408.

898 4. Velasco R, Zharkikh A, Affourtit J, Dhingra A, Cestaro A, Kalyanaraman A et al. The genome of the
899 domesticated apple (*Malus × domestica* Borkh.). Nature Genet. 2010;42:833–839.

900 5. Stehmann C, Pennycook S, Plummer K. Molecular identification of a sexual interloper: the pear
901 pathogen *Venturia pirina*, has sex on apple. Phytopathol. 2001;91:663-541.

902 6. Rossman A, Castlebury L, Aguirre-Hudson B, Berndt R, Edwards. (2647–2651) Proposals to
903 conserve the name *Venturia acerina* against *Cladosporium humile; Venturia borealis* against
904 *Torulama culicola; Venturia carpophila* against *Fusicladium amygdali* and *Cladosporium*
905 *americanum; Sphaerella inaequalis (Venturia inaequalis)* against *Spilocaea pomi, Fumago*
906 *mali, Actinone macrataegi, Cladosporium dendriticum, Asteroma mali,* and *Scolicotrichum*
907 *venosum;* and *Venturia pyrina* against *Helminthosporium pyrorum, Fusicladium virescens, F.*
908 *fuscescens, Cladosporium polymorphum* and *Passalora pomi (Ascomycota: Dothideomycetes)*.
909 Taxon. 2018;67:1209-1211.

910 7. Gonzalez-Dominguez E, Armengol J, Rossi V. Biology and epidemiology of *Venturia* species
911 affecting fruit crops: a review. Front Plant Sci. 2017;8: 1496.
912 8. Jiang S, Park P, Ishii H. Penetration behaviour of *Venturia nashicola* , associated with hydrogen
913 peroxide generation, in Asian and European pear leaves. J Phytopathol. 2014;162: 770-778.
914 9. Chevalier M, Bernard C, Tellier M, Audrain C, Durel CE. Host and non-host interactions of *Venturia*
915 *inaequalis* and *Venturia pirina* on *Pyrus communis* and *Malus x domestica*. Acta Hortic.
916 2004;663: 205-208.
917 10. Lee HA, Lee HY, Seo E, Lee J, Kim SB, Oh S, Choi E, Choi E, Lee SE, Choi D. Current understanding
918 of plant nonhost resistance. Mol Plant-Microbe Interact. 2017a;30:5-5.
919 11. Buron-Moles G, Wisniewski M, Viñas I, Teixidó N, Usall J, Droby S, Torres R. Characterizing the
920 proteome and oxi-proteome of apple in response to a host (Penicillium expansum) and a
921 non-host (Penicillium digitatum) pathogen. J Proteomics. 2015;114:136-151.
922 12. Vilanova L, Vall-Llaura N, Torres R, Usall J, Teixidó N, Larrigaudière C, Giné-Bordonaba J.
923 Penicillium expansum (compatible) and Penicillium digitatum (non-host) pathogen infection
924 differentially alter ethylene biosynthesis in apple fruit. Plant Physiol Biochem. 2017;120:132-
925 143.
926 13. Perchepied L, Chevreau E, Ravon E, Gaillard S, Pelletier S, Bahut M, Berthelot P, Cournol R,
927 Schouten HJ, Vergne E. Successful intergeneric transfer of a major apple scab resistance gene
928 (Rvi6) from apple to pear and precise comparison of the downstream molecular mechanisms
929 of this resistance in both species. BMC Genomics. 2021;22:843.
930 14. Yan Y, Zheng XF, Apaliya MT, Yang HJ, Zhang HY. Transcriptome characterization and expression
931 profile of defense-related genes in pear induced by *Meyerozyma guilliermondii*. Postharvest
932 Biol Technol. 2018;141:63-70.
933 15. Zhang Q, Zhao L, Li B, Gu X, Zhang X, Boateng NS, Zhang H. Molecular dissection of defense
934 response of pears induced by the biocontrol yeast, *Wicherhamomyces anomalus* using
935 transcriptomics and proteomics approaches. Biol Control. 2020;148:104305.

936 16. Wang H, lin J, Chang YH, Jiang CZ. Comparative transcriptomic analysis reveals that
937 ethylene/H2O2-mediated hypersensitive response and programmed cell death determine
938 the compatible interaction of sans pear and *Alternaria alternate.* Front Plant Sci.
939 2017b;8:196.
940 17. Xu M, Yang Q, Boateng NAS, Ahima J, Dou Y, Zhang H. Ultrastructure observation and
941 transcriptome analysis of *Penicillium expansum* invasion in postharvest pears. Postharvest
942 Biol Technol. 2020;165:111198.
943 18. Paris R, Cova V, Pagliarani G, Tartarini S, Konjanc M, Sansavini S. Expression profiling in HcrVf2-
944 transformed apple plants in response to Venturia inaequalis. Tree Genet Genome.
945 2009;5:81–91.
946 19. Cova V, Paris R, Toller C, Patocchi A, Belasco R, Komjanc M. Apple genes involved in the response
947 to Venturia inaequalis and salicylic acid treatment. Sci Hortic. 2017;226:157–72.
948 20. Paris R, Dondini L, Zannini G, Bastia D, Marasco E, Gualdi V, et al. dHPLC efficiency for semi-
949 automated cDNA-AFLP analyses and fragment collection in the apple scab-resistance gene
950 model. Planta. 2012;235:1065–80.
951 21. Gusberti M, Gessler C, Broggini GA. RNA-Seq analysis reveals candidate genes for ontogenic
952 resistance in Malus-Venturia pathosystem. PLoS One. 2013;8:e78457.
953 22. Sikorskaite-Gudziuniene S, Haimi P, Gelvonauskiene D, Stanys V. Nuclear proteome analysis of
954 apple scab cultivar 'Antonovka' accessions in response to apple scab (Venturia inaequalis).
955 Eur J Plant Pathol. 2017;148:771–84.
956 23. Masoodi KZ, Ahmed N, Mir MA, Bhat B, Shafi A, Mansoor S, Rasool RS, Yaseen M, Dar ZA, Mir JI,
957 Andrabi SM, Ganai NA. Comparative transcriptomics unravels new genes imparting scab
958 resistance in apple (Malus x domestica Borkh.). Funct Integr Genomics. 2022; Epub ahead of
959 print.
960 24. Mary-Huard T, Aubert J, Mansouri-Attia N, Sandra O, Daudin JJ. Statistical methodology for the
961 analysis of dye-switch microarray experiments. BMC Bioinformatics. 2008;9:98.

962 25. Van Moerkercke A, Duncan O, Zander M, Šimura J, Broda M, Vanden Bossche R, Lewsey MG,
963 Lama S, Singh KB, Ljung K, Ecker JR, Goossens A, Millar AH, Van Aken O. A
964 MYC2/MYC3/MYC4-dependent transcription factor network regulates water spray-
965 responsive gene expression and jasmonate levels. Proc Natl Acad Sci U S A. 2019;116:23345-
966 23356.
967 26. Wasternack C, Feussner I. The oxylipin pathways: biochemistry and function. Annu Rev Plant Biol.
968 2018;69:363-386.
969 27. Li C, Schilmiller AL, Liu G, Lee GI, Jayanty S, Sageman C, et al. Role of beta-oxidation in jasmonate
970 biosynthesis and systemic wound signaling in tomato. Plant Cell. 2005;17:971-986.
971 28. Seo JS, Koo YJ, Jung C, Yeu SY, Song JT, Kim JK, Choi Y, Lee JS, Do Choi Y. Identification of a novel
972 jasmonate-responsive element in the AtJMT promoter and its binding protein for AtJMT
973 repression. PLoS One. 2013;8:e55482.
974 29. Jeong JS, Jung C, Seo JS, Kim JK, Chua NH. The deubiquitinating enzymes UBP12 and UBP13
975 positively regulate MYC2 levels in jasmonate responses. Plant Cell. 2017;29:1406-1424.
976 30. Birkenbihl RP, Diezel C, Somssich IE. *Arabidopsis* WRKY33 is a key transcriptional regulator of
977 hormonal and metabolic responses toward *Botrytis cinerea* infection. Plant Physiol.
978 2012;159:266-85.
979 31. Kaurilind E, Xu E, Brosché M. A genetic framework for H2O2 induced cell death in *Arabidopsis*
980 *thaliana.* BMC Genomics. 2015;16:837.
981 32. Nurmberg PL, Knox KA, Yun BW, Morris PC, Shafiei R, Hudson A, Loake GJ. The developmental
982 selector AS1 is an evolutionarily conserved regulator of the plant immune response. Proc
983 Natl Acad Sci U.S.A. 2007;104:18795-187800.
984 33. Ali S, Ganai BA, Kamili AN, Bhat AA, Mir ZA, Bhat JA et al. Pathogenesis-related proteins and
985 peptides as promising tools for engineering plants with multiple stress tolerance. Microb Res.
986 2018; 212-213:29-37.

987 34. Li J, Brader G, Palva ET. The WRKY70 transcription factor: a node of convergence for jasmonate-
988 mediated and salicylate-mediated signals in plant defense. Plant Cell. 2004;16:319–331.
989 35. Li J, Brader G, Kariola T, Palva ET. WRKY70 modulates the selection of signaling pathways in plant
990 defense. Plant J. 2006;46:477–491.
991 36. Wang D, Amornsiripanitch N, Dong X. A genomic approach to identify regulatory nodes in the
992 transcriptional network of systemic acquired resistance in plants. PLoS Pathog. 2006;2:e123.
993 37. Li J, Zhong R, Palva ET. WRKY70 and its homolog WRKY54 negatively modulate the cell wall-
994 associated defenses to necrotrophic pathogens in *Arabidopsis*. PLoS One. 2017;12:e0183731.
995 38. Genot B, Lang J, Berriri S, Garmier M, Gilard F, Pateyron S, et al. Constitutively active *Arabidopsis*
996 MAP kinase 3 triggers defense responses involving salicylic acid and SUMM2 resistance
997 protein. Plant Physiol. 2017;174:1238-1249.
998 39. Hu X, Reddy AS. Cloning and expression of a PR5-like protein from *Arabidopsis*: inhibition of
999 fungal growth by bacterially expressed protein. Plant Mol Biol. 1997;34:949-59.
1000 40. Mestre P, Arista G, Piron MC, Rustenholz C, Ritzenthaler C, Merdinoglu D, Chich JF. Identification
1001 of a *Vitis vinifera* endo-β-1,3-glucanase with antimicrobial activity against *Plasmopara*
1002 *viticola*. Mol Plant Pathol. 2017;18:708-719.
1003 41. Zhang SB, Zhang WJ, Zhai HC, Lv YY, Cai JP, Jia F, Wang JS, Hu YS. Expression of a wheat β-1,3-
1004 glucanase in Pichia pastoris and its inhibitory effect on fungi commonly associated with
1005 wheat kernel. Protein Expres Purif. 2019;154:134-139.
1006 42. Santamaria M, Thomson CJ, Read ND, Loake GJ; The promoter of a basic PR1-like gene, AtPRB1,
1007 from *Arabidopsis* establishes an organ-specific expression pattern and responsiveness to
1008 ethylene and methyl jasmonate. Plant Mol Biol. 2001;47:641-52.
1009 43. Truman W, Sreekanta S, Lu Y, Bethke G, Tsuda K, Katagiri F, Glazebrook J. The CALMODULIN-
1010 BINDING PROTEIN60 family includes both negative and positive regulators of plant immunity.
1011 Plant Physiol. 2013;163:1741-1751.

1012 44. Boursiac Y, Lee SM, Romanowsky S, Blank R, Sladek C, Chung WS, Harper JF. Disruption of the
1013 vacuolar calcium-ATPases in *Arabidopsis* results in the activation of a salicylic acid-dependent
1014 programmed cell death pathway. Plant Physiol. 2010;154:1158-71.
1015 45. Huang J, Sun Y, Orduna AR, Jetter R, Li X. The Mediator kinase module serves as a positive
1016 regulator of salicylic acid accumulation and systemic acquired resistance. Plant J. 2019;98:842-
1017 852.
1018 46. Wang W, Tang W, Ma T, Niu D, Jin JB, Wang H, Lin R. A pair of light signaling factors FHY3 and
1019 FAR1 regulates plant immunity by modulating chlorophyll biosynthesis. Journal of Integrative
1020 Plant Biol. 2015;58:91-103.
1021 47. Song JT, Koo YJ, Seo HS, Kim MC, Choi YD, Kim JH. Overexpression of AtSGT1, an *Arabidopsis*
1022 salicylic acid glucosyltransferase, leads to increased susceptibility to *Pseudomonas syringae*.
1023 Phytochemistry. 2008;69:1128-34.
1024 48. Vlot AC, Dempsey DA, Klessig DF. Salicylic acid, a multifaceted hormone to combat disease. Annu
1025 Rev Phytopathol. 2009;47:177-206.
1026 49. Andreasson E, Jenkins T, Brodersen P, Thorgrimsen S, Petersen NH, Zhu S et al. The MAP kinase
1027 substrate MKS1 is a regulator of plant defense responses. EMBO J. 2005;24:2579-89.
1028 50. Xia Y, Yu K, Gao QM, Wilson EV, Navarre D, Kachroo P, Kachroo A. Acyl CoA binding proteins are
1029 required for cuticle formation and plant responses to microbes. Front Plant Sci. 2012;3:224.
1030 51. Boller T, Felix G. A renaissance of elicitors: perception of microbe-associated molecular patterns
1031 and danger signals by pattern recognition receptors. Annu Rev Plant Biol. 2009;60:379-406.
1032 52. Vincill ED, Bieck AM, Spalding EP. Ca(2+) conduction by an amino acid-gated ion channel related
1033 to glutamate receptors. Plant Physiol. 2012;159:40-46.
1034 53. Hou C, Tian W, Kleist T, He K, Garcia V, Bai F, Hao Y, Luan S, Li L. DUF221 proteins are a family of
1035 osmosensitive calcium-permeable cation channels conserved across eukaryotes. Cell Res.
1036 2014;24:632-635.

1037 54. Fonseca JP, Mysore KS. Genes involved in nonhost disease resistance as a key to engineer durable
1038 resistance in crops. Plant Sci. 2019;279:108-116.
1039 55. Ronzier E, Corratgé-Faillie C, Sanchez F, Prado K, Brière C, Leonhardt N, Thibaud JB, Xiong TC.
1040 CPK13, a noncanonical Ca2+-dependent protein kinase, specifically inhibits KAT2 and KAT1
1041 shaker K+ channels and reduces stomatal opening. Plant Physiol. 2014;166:314-26.
1042 56. Zou JJ, Li XD, Ratnasekera D, Wang C, Liu WX, Song LF, Zhang WZ, Wu WH. *Arabidopsis* CALCIUM-
1043 DEPENDENT PROTEIN KINASE8 and CATALASE3 function in abscisic acid-mediated signaling
1044 and H2O2 homeostasis in stomatal guard cells under drought stress. Plant Cell.
1045 2015;27:1445-1460.
1046 57. Förster S, Schmidt LK, Kopic E, Anschütz U, Huang S, Schlücking K, et al. Wounding-induced
1047 stomatal closure requires jasmonate-mediated activation of GORK K(+) channels by a Ca(2+)
1048 sensor-kinase CBL1-CIPK5 complex. Dev Cell. 2019;48:87-99.e6.
1049 58. Kadota Y, Shirasu K, Zipfel C. Regulation of the NADPH oxidase RBOHD during plant immunity.
1050 Plant Cell Physiol. 2015;56: 1472–1480.
1051 59. Adachi H, Yoshioka H. Kinase-mediated orchestration of NADPH oxidase in plant immunity. Brief
1052 Funct Genomics. 2015;14:253-259.
1053 60. Zhai L, Sun C, Feng Y, Li D, Chai X, Wang L, Sun Q, et al. AtROP6 is involved in reactive oxygen
1054 species signaling in response to iron-deficiency stress in *Arabidopsis thaliana*. FEBS Lett.
1055 2018;592:3446-3459.
1056 61. Gao X, Chen X, Lin W, Chen S, Lu D, Niu Y, Li L, Cheng C, McCormack M, Sheen J, Shan L, He P.
1057 Bifurcation of *Arabidopsis* NLR immune signaling via Ca^{2+}-dependent protein kinases. PLoS
1058 Pathog. 2013;9:e1003127.
1059 62. Qi J, Wang J, Gong Z, Zhou JM. Apoplastic ROS signaling in plant immunity. Curr Opin Plant Biol.
1060 2017;38:92-100.

1061 63. Bourdais G, Burdiak P, Gauthier A, Nitsch L, Salojärvi J, Rayapuram C et al. CRK consortium large-
1062 scale phenomics identifies primary and fine-tuning roles for CRKs in responses related to
1063 oxidative stress. PLoS Genet. 2015;11:e1005373.
1064 64. Sun T, Nitta Y, Zhang Q, Wu D, Tian H, Lee JS, Zhang Y. Antagonistic interactions between two
1065 MAP kinase cascades in plant development and immune signaling. EMBO Rep.
1066 2018;19:e45324.
1067 65. O'Brien JA, Daudi A, Butt VS, Bolwell GP. Reactive oxygen species and their role in plant defence
1068 and cell wall metabolism. Planta. 2012;236:765-779.
1069 66. Brosché M, Blomster T, Salojärvi J, Cui F, Sipari N, Leppälä J et al. Transcriptomics and functional
1070 genomics of ROS-induced cell death regulation by RADICAL-INDUCED CELL DEATH1. PLoS
1071 Genet. 2014;10:e1004112.
1072 67. Cheng YT, Li Y, Huang S, Huang Y, Dong X, Zhang Y, Li X. Stability of plant immune-receptor
1073 resistance proteins is controlled by SKP1-CULLIN1-F-box (SCF)-mediated protein degradation.
1074 Proc Natl Acad Sci U.S.A. 2011;108:14694-14699.
1075 68. Coll NS, Vercammen D, Smidler A, Clover C, Van Breusegem F, Dangl JL, Epple P. *Arabidopsis* type
1076 I metacaspases control cell death. Science. 2010;330:1393-1397.
1077 69. Lema-Asqui S, Vercammen D, Serrano I, Valls M, Rivas S, Van Breusegem F, et al. AtSERPIN1 is an
1078 inhibitor of the metacaspase AtMC1-mediated cell death and autocatalytic processing in
1079 planta. New Phytol. 2018;218:1156-1166.
1080 70. Kawasaki T, Nam J, Boyes DC, Holt BF, Hubert DA, Wiig A, Dangl JL. A duplicated pair of
1081 *Arabidopsis* RING-finger E3 ligases contribute to the RPM1-and RPS2-mediated
1082 hypersensitive response. Plant J. 2005;44: 258-270.
1083 71. Luo H, Laluk K, Lai Z, Veronese P, Song F, Mengiste T. The *Arabidopsis* Botrytis Susceptible1
1084 interactor defines a subclass of RING E3 ligases that regulate pathogen and stress responses.
1085 Plant Physiol. 2010;154:1766-1782.

1086 72. Huby E, Napier JA, Baillieul F, Michaelson LV, Dhondt-Cordelier S. Sphingolipids: towards an
1087 integrated view of metabolism during the plant stress response. New Phytol. 2020;225:659-
1088 670.
1089 73. Saucedo-Garcia M, Guevara-Garcia A, Gonzalez-Solis A, Cruz-Garcia F, VazquezSantana S,
1090 Markham JE, et al. MPK6, sphinganine and the LCB2a gene from serine palmitoyltransferase
1091 are required in the signaling pathway that mediates cell death induced by long chain bases in
1092 *Arabidopsis*. New Phytol. 2011;191:943–957.
1093 74. Veley KM, Maksaev G, Frick EM, January E, Kloepper SC, Haswell ES. *Arabidopsis* MSL10 has a
1094 regulated cell death signaling activity that is separable from its mechanosensitive ion channel
1095 activity. Plant Cell. 2014;26:3115-3131.
1096 75. Guerringue Y, Thomine S, Frachisse JM. Sensing and transducing forces in plants with MSL10 and
1097 DEK1 mechanosensors. FEBS Lett. 2018;592:1968-1979.
1098 76. Zhao C, Nie H, Shen Q, Zhang S, Lukowitz W, Tang D. EDR1 physically interacts with MKK4/MKK5
1099 and negatively regulates a MAP kinase cascade to modulate plant innate immunity. PLoS
1100 Genet. 2014;10:e1004389.
1101 77. Lee MH, Jeon HS, Kim HG, Park OK. An *Arabidopsis* NAC transcription factor NAC4 promotes
1102 pathogen-induced cell death under negative regulation by microRNA164. New Phytol.
1103 2017b;214:343-360.
1104 78. Najafi J, Brembu T, Vie AK, Viste R, Winge P, Somssich IE, Bones AM. PAMP-INDUCED SECRETED
1105 PEPTIDE 3 modulates immunity in *Arabidopsis*. J Exp Bot. 2020;71:850-864.
1106 79. Khafif M, Balagué C, Huard-Chauveau C, Roby D. An essential role for the VASt domain of the
1107 *Arabidopsis* VAD1 protein in the regulation of defense and cell death in response to
1108 pathogens. PLoS One. 2017;12:e0179782.
1109 80. Simon C, Langlois-Meurinne M, Didierlaurent L, Chaouch S, Bellvert F, Massoud K, et al. The
1110 secondary metabolism glycosyltransferases UGT73B3 and UGT73B5 are components of redox

1111 status in resistance of *Arabidopsis* to *Pseudomonas syringae* pv. *tomato*. Plant Cell Environ.
1112 2014;37:1114-1129.
1113 81. Bacete L, Mélida H, Miedes E, Molina A. Plant cell wall-mediated immunity: cell wall changes
1114 trigger disease resistance responses. Plant J. 2018;93:614-636.
1115 82. Miedes E, Vanholme R, Boerjan W, Molina A. The role of the secondary cell wall in plant
1116 resistance to pathogens. Front Plant Sci. 2014;5:358.
1117 83. Fich EA, Segerson NA, Rose JK. The plant polyester cutin: biosynthesis, structure, and biological
1118 roles. Ann Rev Plant Biol. 2016;67:207-233.
1119 84. Lim GH, Singhal R, Kachroo A, Kachroo P. Fatty acid- and lipid-mediated signaling in plant defense.
1120 Annu Rev Phytopathol. 2017;55:505-536.
1121 85. Joubès J, Raffaele S, Bourdenx B, Garcia C, Laroche-Traineau J, Moreau P, Domergue F, Lessire R.
1122 The VLCFA elongase gene family in *Arabidopsis thaliana*: phylogenetic analysis, 3D modelling
1123 and expression profiling. Plant Mol Biol. 2008;67:547-66.
1124 86. Lee SB and Suh MC. Advances in the understanding of cuticular waxes in *Arabidopsis thaliana* and
1125 crop species. Plant Cell Rep. 2015;34:557-572.
1126 87. Li Y, Beisson F, Koo AJ, Molina I, Pollard M, Ohlrogge J. Identification of acyltransferases required
1127 for cutin biosynthesis and production of cutin with suberin-like monomers. Proc Natl Acad Sci
1128 U.S.A. 2007;104:18339-18344.
1129 88. Yeats TH, Huang W, Chatterjee S, Viart HM, Clausen MH, Stark RE, Rose JK. Tomato Cutin
1130 Deficient 1 (CD1) and putative orthologs comprise an ancient family of cutin synthase-like
1131 (CUS) proteins that are conserved among land plants. Plant J. 2014;77:667-675.
1132 89. Cui F, Brosche M, Lehtonen MT, Amiryousefi A, Xu E, Punkkinen M, Valkonen JPT, Fujii H,
1133 Overmyer K. Dissecting abscisic acid signaling pathways involved in cuticle formation. Mol
1134 Plant. 2016;9: 926-938.
1135 90. Yang L, Wen KS, Ruan X, Zhao YX, Wei F, Wang Q**.** Response of plant secondary metabolites to
1136 environmental factors. Molecules. 2018;23i:e762.

1137 91. Tetali S. Terpenes and isoprenoids: a wealth of compounds for global use. Planta. 2019;249:1-8.
1138 92. Wang K, Senthil-Kumar M, Ryu CM, Kang L, Mysore KS. Phytosterols play a key role in plant innate
1139 immunity against bacterial pathogens by regulating nutrient efflux into the apoplast. Plant
1140 Physiol. 2012;158:1789-1802.
1141 93. Falcone Ferreyra ML, Emiliani J, Rodriguez EJ, Campos-Bermudez VA, Grotewold E, Casati P. The
1142 identification of maize and *Arabidopsis* type I FLAVONE SYNTHASEs links flavones with
1143 hormones and biotic interactions. Plant Physiol. 2015;169:1090-107.
1144 94. Wang N, Xu H, Jiang S, Zhang Z, Lu N, Qiu H, Qu C, Wang Y, Wu S, Chen X. MYB12 and MYB22 play
1145 essential roles in proanthocyanidin and flavonol synthesis in red-fleshed apple (*Malus*
1146 *sieversii* f. *niedzwetzkyana*). Plant J. 2017a;90:276-292.
1147 95. Zhai R, Zhao Y, Wu M, Yang J, Li X, Liu H, Wu T, Liang F, Yang C, Wang Z, Ma F, Xu L. The MYB
1148 transcription factor PbMYB12b positively regulates flavonol biosynthesis in pear fruit. BMC
1149 Plant Biol. 2019;19:85.
1150 96. Wang XC, Wu J, Guan ML, Zhao CH, Geng P, Zhao Q. *Arabidopsis* MYB4 plays dual roles in
1151 flavonoid biosynthesis. Plant J. 2020;101:637-652.
1152 97. Fernández-Pérez F, Vivar T, Pomar F, Pedreño MA, Novo-Uzal E. Peroxidase 4 is involved in
1153 syringyl lignin formation in *Arabidopsis thaliana*. J Plant Physiol. 2015a;175:86-94.
1154 98. Zhao Q, Nakashima J, Chen F, Yin Y, Fu C, Yun J, Shao H, Wang X, Wang ZY, Dixon RA. Laccase is
1155 necessary and nonredundant with peroxidase for lignin polymerization during vascular
1156 development in *Arabidopsis*. Plant Cell. 2013;25:3976-3987.
1157 99. Cosio C, Ranocha P, Francoz E, Burlat V, Zheng Y, Perry SE, Ripoll JJ, Yanofsky M, Dunand C. The
1158 class III peroxidase PRX17 is a direct target of the MADS-box transcription factor AGAMOUS-
1159 LIKE15 (AGL15) and participates in lignified tissue formation. New Phytol. 2017;213:250-263.
1160 100. Tokunaga N, Kaneta T, Sato S, Sato Y. Analysis of expression profiles of three peroxidase genes
1161 associated with lignification in *Arabidopsis thaliana*. Physiol Plantarum. 2009;136:237-249.

1162 101. Fernández-Pérez F, Pomar F, Pedreño MA, Novo-Uzal E. The suppression of AtPrx52 affects
1163 fibers but not xylem lignification in *Arabidopsis* by altering the proportion of syringyl units.
1164 Physiol Plantarum. 2015b;154:395-406.
1165 102. Vilanova L, Teixidó N, Torres R, Usall J, Viñas I. The infection capacity of *P. expansum* and *P.*
1166 *digitatum* on apples and histochemical analysis of host response. International Journal of
1167 Food Microbiol. 2012;157:360-367.
1168 103. Fink W, Haug M, Deising H, Mendgen K. Early defence responses of cowpea *(Vigna sinensis* L.)
1169 induced by non-pathogenic rust fungi. Planta. 1991;185:246-254.
1170 104. Yu Y, Yu Y, Cui N, Ma L, Tao R, Ma Z, Meng X, Fan H. Lignin biosynthesis regulated by CsCSE1 is
1171 required for Cucumis sativus defence to Podosphaera xanthii. Plant Physiol Biochem.
1172 2022;186:88-98.
1173 105. Ranade SS, Seipel G, Gorzsás A, García-Gil MR. Enhanced lignin synthesis and ecotypic variation
1174 in defense-related gene expression in response to shade in Norway spruce. Plant Cell
1175 Environ. 2022;45:2671-2681.
1176 106. Song PP, Zhao J, Liu ZL, Duan YB, Hou YP, Zhao CQ, Wu M, Wei M, Wang NH, Lv Y, Han ZJ.
1177 Evaluation of antifungal activities and structure-activity relationships of coumarin derivatives.
1178 Pest Manag. Sci. 2017;73:94-101.
1179 107. Giesemann A, Biehl B, Lieberei R. Identification of scopoletin as a phytoalexin of the rubber tree
1180 *Hevea brasiliensis*. J Phytopathol. 1986;117:373–376.
1181 108. Muroi A, Ishihara A, Tanaka C, Ishizuka A, Takabayashi J, Miyoshi H, Nishioka T. Accumulation of
1182 hydroxycinnamic acid amides induced by pathogen infection and identification of agmatine
1183 coumaroyltransferase in *Arabidopsis thaliana*. Planta. 2009;230:517-527.
1184 109. Dobritzsch M, Lübken T, Eschen-Lippold L, Gorzolka K, Blum E, Matern A et al. MATE
1185 transporter-dependent export of hydroxycinnamic acid amides. Plant Cell. 2016;28:583-96.
1186 110. Celoy RM, VanEtten HD. (+)-Pisatin biosynthesis: from (-) enantiomeric intermediates via an
1187 achiral 7,2'-dihydroxy-4',5'-methylenedioxyisoflav-3-ene. Phytochem. 2014;98:120-127.

1188 111. Vorwieger A, Gryczka C, Czihal A, Douchkov D, Tiedemann J, Mock HP, et al. Iron assimilation
1189 and transcription factor controlled synthesis of riboflavin in plants. Planta. 2007;226:147-
1190 158.
1191 112. Trapalis M, Li SF, Parish RW. The *Arabidopsis* GASA10 gene encodes a cell wall protein strongly
1192 expressed in developing anthers and seeds. Plant Sci. 2017;260:71-79.
1193 113. Yamauchi Y, Hasegawa A, Mizutani M, Sugimoto Y. Chloroplastic NADPH-dependent alkenal/one
1194 oxidoreductase contributes to the detoxification of reactive carbonyls produced under
1195 oxidative stress. FEBS Lett. 2012;586:1208-1213.
1196 114. Segond D, Dellagi A, Lanquar V, Rigault M, Patrit O, Thomine S, Expert D. NRAMP genes function
1197 in *Arabidopsis thaliana* resistance to *Erwinia chrysanthemi* infection. Plant J. 2009;58:195-
1198 207.
1199 115. Lee MW, Jelenska J, Greenberg JT. *Arabidopsis* proteins important for modulating defense
1200 responses to *Pseudomonas syringae* that secrete HopW1-1. Plant J. 2008;54:452-445.
1201 116. Hong GJ, Xue XY, Mao YB, Wang LJ, Chen XY. *Arabidopsis* MYC2 interacts with DELLA proteins in
1202 regulating sesquiterpene synthase gene expression. Plant Cell. 2012;24:2635-2648.
1203 117. Rodriguez-Saona CR, Polashock J, Malo EA. Jasmonate-mediated induced volatiles in the
1204 American cranberry, *Vaccinium macrocarpon*: from gene expression to organismal
1205 interactions. Front Plant Sci. 2013;4:115.
1206 118. Simanshu DK, Zhai X, Munch D, Hofius D, Markham JE, Bielawski J, et al. *Arabidopsis* accelerated
1207 cell death 11, ACD11, is a ceramide-1-phosphate transfer protein and intermediary regulator
1208 of phytoceramide levels. Cell Rep. 2014;6:388-399.
1209 119. Fink L, Kwapiszewska G, Wilhelm J, Bohle RM. Laser-microdissection for cell type- and
1210 compartment-specific analyses on genomic and proteomic level. Exp Toxicol Pathol. 2006;57
1211 Suppl 2:25-259.
1212 120. Gill US, Lee S, Mysore KS. Host versus nonhost resistance: distinct wars with similar arsenals.
1213 Phytopathol. 2015;105:580-587.

1214 121. Pieterse CM, Van der Does D, Zamioudis C, Leon-Reyes A, Van Wees SC. Hormonal modulation
1215 of plant immunity. Annu Rev Cell Dev Biol. 2012;28:489-521.
1216 122. Tsuda K, Sato M, Stoddard T, Glazebrook J, Katagiri F. Network properties of robust immunity in
1217 plants. PLoS Genet. 2009;5(12):e1000772.
1218
1219 123. Faize M, Malnoy M, Dupuis F, Chevalier M, Parisi L, Chevreau E. Chitinases of *Trichoderma*
1220 *atroviridae* induce scab resistance and some metabolic changes in two cultivars of apple.
1221 Phytopathol. 2003;93:1496-1504.
1222 124. Leblay C, Chevreau E, Raboin LM. Adventitious shoot regeneration from in vitro leaves of several
1223 pear cultivars (*Pyrus communis* L.). Plant Cell Tissue Organ Cult. 1991;25:99-105.
1224 125. Lespinasse Y, Durel CE, Parisi L, Laurens F, Chevalier M, Pinet C. A European project: D.A.R.E.
1225 Durable apple resistance in Europe. Acta Hortic. 2000;538:197–200.
1226 126. Chevalier M, Tellier M, Lespinasse Y, Bruynincks M, Georgeault S. Behaviour studies of new
1227 races of *Venturia pirina* isolated from 'Conference' cultivar on a range of pear cultivars. Acta
1228 Hortic. 2008a;800:817-824.
1229 127. Parisi L, Lespinasse Y. Pathogenicity of *Venturia inaequalis* strains of race 6 on apple clone
1230 (*Malus sp*.). Plant Dis. 1996;80: 1179-1183.
1231 128. Chevalier M, Tellier M, Lespinasse Y, Caffier V. How to optimize the *Venturia* pirina inoculation
1232 on pear leaves in greenhouse conditions? Acta Hortic. 2008b;800: 913-920.
1233 129. Chevalier M, Lespinasse Y, Renaudin S. A microscopic study of different classes of symptoms
1234 coded by the *Vf* gene in apple resistance to scab (*Venturia inaequalis*). Plant Pathol. 1991;40:
1235 249–256.
1236 130. Hoch HC, Galvani CD, Szarowski DH, Turner JN. Two new fluorescent dyes applicable for
1237 visualization of fungal cell walls. Mycologia. 2005;97: 580-588.

1238 131. Depuydt S, Trenkamp S, Fernie AR, Elftieh S, Renou J-P, Vuylsteke M, Holster M, Vereecke D. An
1239 integrated genomic approach to define niche establishment by *Rhodococcus fascians* . Plant
1240 Physiol. 2009;149: 1366–1386.
1241 132. Celton JM, Gaillard S, Bruneau M, Pelletier S, Aubourg S, Martin-Magniette ML, Navarro L,
1242 Laurens F, Renou JP. Widespread anti-sense transcription in apple is correlated with siRNA
1243 production and indicates a large potential for transcriptional and/or post-transcriptional
1244 control. New Phytol. 2014;203:287-99.
1245 133. Smyth G. “limma: linear models for microarray data”, in Bioinformatics and Computational
1246 Biology Solutions Using R and Bioconductor, eds Gentleman R., Carey V., Dudoit S., Irizarry R.,
1247 Huber W. New York, NY: Springer, 397–420.
1248 134. Ritchie ME, Phipson B, Wu D, Hu Y, Law CW, Shi W, Smyth GK. limma powers differential
1249 expression analyses for RNA-sequencing and microarray studies. Nucleic Acids Res.
1250 2015;43:e47.135. Pelletier S. AnaDiff: A tool for differential analysis of microarrays and
1251 RNAseq (v4.3). 2022. Zenodo. https://doi.org/10.5281/zenodo.6477918
1252 135. Pelletier S. AnaDiff: A tool for differential analysis of microarrays and RNAseq (v4.3). 2022.
1253 Zenodo. https://doi.org/10.5281/zenodo.6477918
1254 136. Berardini TZ, Reiser L, Li D, Mezheritsky Y, Muller R, Strait E, Huala E. The *Arabidopsis*
1255 information resource: Making and mining the "gold standard" annotated reference plant
1256 genome. Genesis. 2015;53:474-85.
1257 137. Provart, N., Zhu, T. A Browser-based Functional Classification SuperViewer for Arabidopsis
1258 Genomics. Currents in Computational Molecular Biology. 2003;271-272.
1259 138. Thimm O, Bläsing O, Gibon Y, Nagel A, Meyer S, Krüger P, Selbig J, Müller LA, Rhee SY, Stitt M.
1260 MAPMAN: a user-driven tool to display genomics data sets onto diagrams of metabolic
1261 pathways and other biological processes. Plant J. 2004;37:914-939.
1262 139. Pfaffl MW. A new mathematical model for relative quantification in real-time RT-PCR. Nucleic
1263 Acids Res. 2001;29, e45.

1264 140. Livak KJ, Schmittgen TD. Analysis of relative gene expression data using real-time quantitative
1265 PCR and the 2−ΔΔCT method. Methods. 2001;25:402-408.
1266 141. Vandesompele, J, De Preter, K, Pattyn, F, Poppe, B, Van Roy, N, De Paepe, A et al. Accurate
1267 normalization of real-time quantitative RT-PCR data by geometric averaging of multiple
1268 internal control genes. Genome Biol. 2002;3(7):00341-003411.
1269 142. Vergne E. Expression data for apple Rvi6 host resistance and nonhost resistance against scab.
1270 2020. https://www.ncbi.nlm.nih.gov/geo/query/acc.cgi?acc=GSE159179
1271 143. Vergne E. Expression data for 1) pear host resistance allowed by transgenic expression of apple
1272 Rvi6 resistance gene and 2) nonhost resistance against scab. 2020.
1273 https://www.ncbi.nlm.nih.gov/geo/query/acc.cgi?acc=GSE159180
1274

1275 ## Figure legends

1276

1277 **Fig. 1**: **Macro- and microscopic observations of nonhost interactions.**
1278 *V. pyrina* VP102 strain / pear 'Conference' (A) and *V. inaequalis* EUB05 strain / apple 'Gala' (B) 21
1279 days symptoms are shown as classical ones of susceptible host interactions, to compare to nonhost
1280 ones. Binocular observation 21 days after *V. inaequalis* EUB05 strain inoculation on 'Conference' (C)
1281 and (D) and *V. pyrina* VP102 strain inoculation on 'Gala' (E). Wide field fluorescence observations of:
1282 'Conference' 3 days (F) and 14 days (H and J) after *V. inaequalis* EUB05 strain inoculation, 'Gala' 3
1283 days (G) and 14 days (I and K) after *V. pyrina* VP102 strain inoculation. Ap: appressorium, C: conidia,
1284 Gf: germination filament, Pp: pin point

1285

1286 **Fig. 2**: **Functional categories of DEGs at 24 or 72 hpi during pear response to *V. inaequalis*.**
1287 The 1845 DEGs with TAIR names have been classified according to MapMan functional categories. In
1288 order to highlight the enriched ones, the numbers of DEGs per category have been normalized to the

1289 numbers of *Arabidopsis* genes in each MapMan category and bootstraps have been done to provide
1290 a confidence estimate for the accuracy of the output.
1291
1292 **Fig. 3: DEGs involved in hormonal pathways during pear/*V. inaequalis* nonhost interaction**.
1293 A: DEGs involved in JA pathway; B: DEGs involved in SA pathway. Genes written in red are induced,
1294 genes written in blue are repressed. ACA11: autoinhibited $Ca2^{+}$-ATPase, calmodulin-activated $Ca2^{+}$
1295 pumps at the plasma membrane, endoplasmic reticulum, and vacuole. ACBP6: acyl-CoA-binding
1296 protein. ACX4: acyl-CoA-oxidase1. AS1/MYB91: Asymmetric leaves 1 transcription factor, CAMTA1:
1297 calmodulin-binding transcription activator, CBP60a: calmodulin-binding protein 60a, EDS1: enhanced
1298 disease suceptibility 1. FAR1: FAR-red impaired response 1. G-box: cis-element in the promoter. JAZ:
1299 jasmonate-zim domain protein, JMT: jasmonic acid carboxyl methyltransferase. LOX: lipoxygenase,
1300 MES1: methylesterase 1. MFP2: multifunctional protein 2. MKS1: MAP kinase substrate 1. MYC2:
1301 transcription factor. NINJA: novel interactor of JAZ. PAD4: phytoalexin deficient 4. UGT74F1:
1302 glucosyltransferase. PR1-like (with ATPRB1), PR2, PR3, PR4 (HEL and ATEP3), PR5, PR12:
1303 pathogenesis-related proteins. ST2A: sulfotransferase 2A. TPL: TOPLESS co-repressor. UBP12:
1304 ubiquitin-specific protease 12. WRKY: transcription factor.
1305
1306 **Fig. 4**: **Scenario of major events observed at three first days of pear/*V. inaequalis* nonhost**
1307 **interaction.**
1308 On the left side, events observed in a typical cell, on the right side, events observed in guard cells of a
1309 stomata. A: apoplasm, AP: appressorium, C: cuticle, CBL1: calcineurin B-like protein 1, CDPK: Ca_2^{+}-
1310 dependent protein kinases, CRK: cysteine-rich receptor-like kinase, CY: cytoplasm, CW: cell wall, HAA:
1311 hydroxycinnamic acid amines, HR: hypersensitive response, JA: jasmonic acid, MB: plasma
1312 membrane, LCB: Long Chain/sphingoid Base components, MPK6: Mitogen activated protein kinase 6,
1313 MSL10: mechano-sensitive like 10, N: nucleus, PH: penetration hypha, PR: pathogenesis related

1314 proteins, RBOHB: respiratory burst oxidase homolog B, ROS: reactive oxygen species, S: stomata, SA:
1315 salycilic acid, SC: simple coumarins, SP: spore.
1316
1317 **Fig. 5: Main DEGs involved in cutin and wax biosynthesis during pear/V. inaequalis nonhost**
1318 **interaction**.
1319 In green the chloroplast, in brown the endoplastic reticulum (ER) and in yellow the nucleus. Genes
1320 written in red are induced, genes written in blue are repressed. FAS: Fatty Acid Synthase complex to
1321 which belong ACCD (carboxytransferase beta subunit of the Acetyl-CoA carboxylase complex), FabG
1322 (β-ketoacyl ACP-reductase) and MOD1 (enoyl-ACP-reductase) functions. FAE: fatty acid elongase
1323 complex. KCS4 (3-ketoacyl-CoA synthase 4) and ECR/CER10 (trans-2-enoyl-CoA reductase) belong to
1324 the FAE complex. CER1 (octadecanal decarbonylase) and CER3 are implicated in aldehydes (CER1)
1325 and alkanes (CER1 and 3) generation in waxes biosynthesis. In cutin monomers synthesis, the ω-
1326 hydroxylation of C16:0 and C18:1 is catalyzed by cytochrome P450 monooxygenase (CYP86A) and
1327 LACS-encoded acyl-CoA synthetase may be required either to synthesize 16-hydroxy 16:0-CoA, a
1328 substrate for ω-hydroxylase, or for membrane transfer of monomers. Finally, the mature
1329 monoacylglycerol cutin monomers are generated by transfer of the acyl group from acyl-CoA to
1330 glycerol-3-phosphate by glycerol-3-phosphate acyltransferase (GPAT) enzymes such as GPAT8. Some
1331 GDSL-lipases enzyme (such as At1g28600, At1g28660, At1g54790, At3g16370, At3g48460, AtCUS4:
1332 At4g28780, At5g14450) are then functioning as cutin synthase and polymerize cutin
1333 monoacylglycerols. Transcription factors such as MYB16 and SHN1 are positive regulators of wax and
1334 cutin biosynthesis. Adapted from Xia et al., 2009, [83] and [84].
1335
1336 **Fig. 6: Main DEGs involved in the phenylpropanoid pathway during Pear / *V. inaequalis* nonhost**
1337 **interaction.**
1338 Genes framed in red are induced, genes frames in blue are repressed. Framed in black, the detail of
1339 genes involved in flavonoids production and found in this interaction. Abbreviations: 4CL, 4-

1340 coumarate-CoA ligase; AACT, anthocyanin 5-aromatic acyltransferase; ANR, anthocyanidin reductase;
1341 ANS, anthocyanin synthase; BGLC or BGLU, β-glucosidases; C3H, coumarate 3-hydroxylase; C4H,
1342 cinnamate 4-hydroxylase; CAD, cinnamyl alcohol dehydrogenase; CCoAOMT, caffeoyl-CoA O-
1343 methyltransferase; CCR, cinnamoyl-CoA reductase; CHI, chalcone isomerase; CHS, chalcone synthase;
1344 COMT, caffeic acid 3-O-methyltransferase; CPK, calcium-dependent protein kinase ; DFR,
1345 dihydroflavonol reductase; DMR6, downy mildiou resistant 6; F3H, flavanone 3-hydroxylase; F3'H
1346 flavonoid 3'-hydroxylase; FLS, flavonol synthase; FNS, flavone synthase; GGT1, gamma-glutamyl
1347 transpeptidase 1; GT, glucosyl transferase; HCT, hydroxycinnamoyl-CoA shikimate/quinate
1348 hydroxycinnamoyl transferase; LAC, laccase; LAR, leucoanthocyanidin reductase; OMT1, O-
1349 methyltransferase 1; PAL, phenylalanine ammonia-lyase; PER or PRX, peroxidase; TT7, transparent
1350 testa 7; UGFT, UDP-glucose flavonoid-3-O-glucosyltransferase; UGT71D1, UDP-glycosyltransferase
1351 71D1.

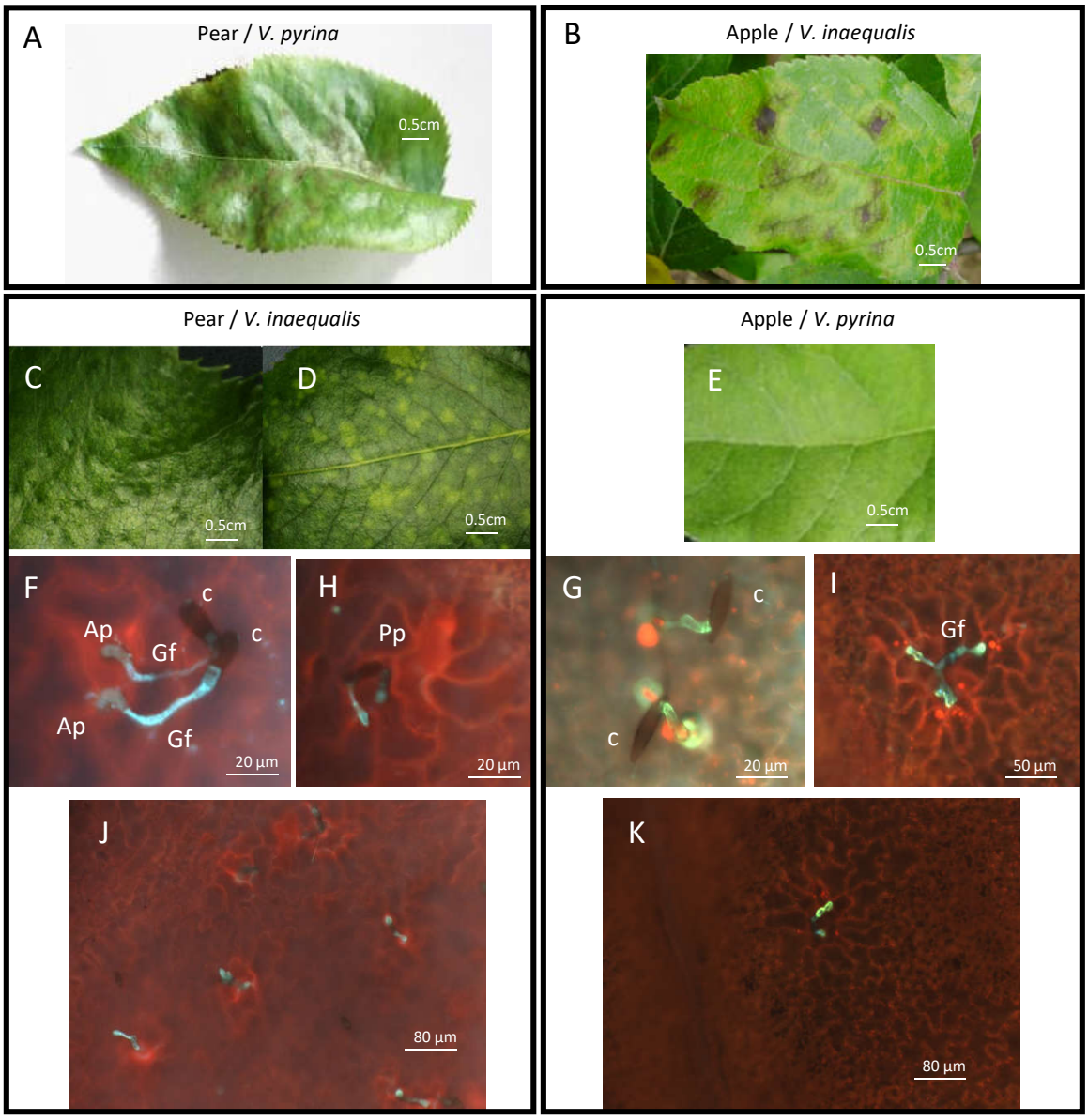
A
Pear / V. pyrina
0.5cm
B
Apple / V. inaequalis
0.5cm
Pear / V. inaequalis
C
0.5cm
D
0.5cm
Apple / V. pyrina
E
0.5cm
F
c
Ap
Gf
c
Ap
Gf
20 µm
H
Pp
20 µm
G
c
c
20 µm
I
Gf
50 µm
J
80 µm
K
80 µm

Fig. 1

Number of DEG	Frequence of DEG normalize to the number of Arabidopsis genes in each class in MapMan	± Bootstrap standard deviation	P_value (>0,05 in bold)	Fonctional class
4	4.55	*2.156*	**8.385e-03**	polyamine metabolism (Input set freq.: 0; 0)
17	3.91	*0.883*	**8.663e-07**	TCA / org transformation (Input set freq.: 0; 0)
5	3.25	*1.476*	**0.013**	Biodegradation of Xenobiotics (Input set freq.: 0; 0)
7	2.65	*1*	**0.011**	tetrapyrrole synthesis (Input set freq.: 0; 0)
5	2.27	*1.019*	**0.045**	C1-metabolism (Input set freq.: 0; 0)
47	1.92	*0.275*	**7.666e-06**	secondary metabolism (Input set freq.: 0.02; 0.01)
8	1.84	*0.698*	**0.039**	glycolysis (Input set freq.: 0; 0)
137	1.83	*0.154*	**2.650e-12**	signalling (Input set freq.: 0.07; 0.04)
12	1.76	*0.578*	**0.021**	minor CHO metabolism (Input set freq.: 0; 0)
3	1.76	*0.875*	0.153	OPP (Input set freq.: 0; 0)
92	1.64	*0.135*	**1.012e-06**	transport (Input set freq.: 0.04; 0.03)
9	1.62	*0.54*	0.052	major CHO metabolism (Input set freq.: 0; 0)
38	1.61	*0.247*	**1.191e-03**	lipid metabolism (Input set freq.: 0.02; 0.01)
16	1.61	*0.364*	**0.019**	nucleotide metabolism (Input set freq.: 0; 0)
22	1.54	*0.322*	**0.013**	amino acid metabolism (Input set freq.: 0.01; 0)
45	1.51	*0.221*	**1.559e-03**	hormone metabolism (Input set freq.: 0.02; 0.01)
66	1.44	*0.185*	**6.346e-04**	cell (Input set freq.: 0.03; 0.02)
16	1.41	*0.329*	**0.041**	PS (Input set freq.: 0; 0)
2	1.4	*0.78*	0.253	N-metabolism (Input set freq.: 0; 0)
1	1.4	*1.281*	0.363	S-assimilation (Input set freq.: 0; 0)
1	1.4	*1.017*	0.363	gluconeogenesis / glyoxylate cycle (Input set freq.: 0; 0)
42	1.39	*0.217*	**6.642e-03**	cell wall (Input set freq.: 0.02; 0.01)
231	1.38	*0.084*	**7.613e-08**	RNA (Input set freq.: 0.12; 0.09)
93	1.37	*0.136*	**3.589e-04**	stress (Input set freq.: 0.05; 0.03)
116	1.32	*0.114*	**3.215e-04**	misc (Input set freq.: 0.06; 0.04)
1	1.3	*0.802*	0.369	fermentation (Input set freq.: 0; 0)
15	1.3	*0.353*	0.064	redox (Input set freq.: 0; 0)
45	1.04	*0.144*	0.060	development (Input set freq.: 0.02; 0.02)
256	0.96	*0.053*	**0.022**	protein (Input set freq.: 0.13; 0.14)
4	0.89	*0.422*	0.196	Co-factor and vitamine metabolism (Input set freq.: 0; 0)
6	0.72	*0.28*	0.113	mitochondrial electron transport / ATP synthesis (Input set freq.: 0; 0)
473	0.72	*0.029*	**6.015e-20**	not assigned (Input set freq.: 0.25; 0.35)
30	0.17	*0.028*	**1.079e-44**	DNA (Input set freq.: 0.01; 0.09)

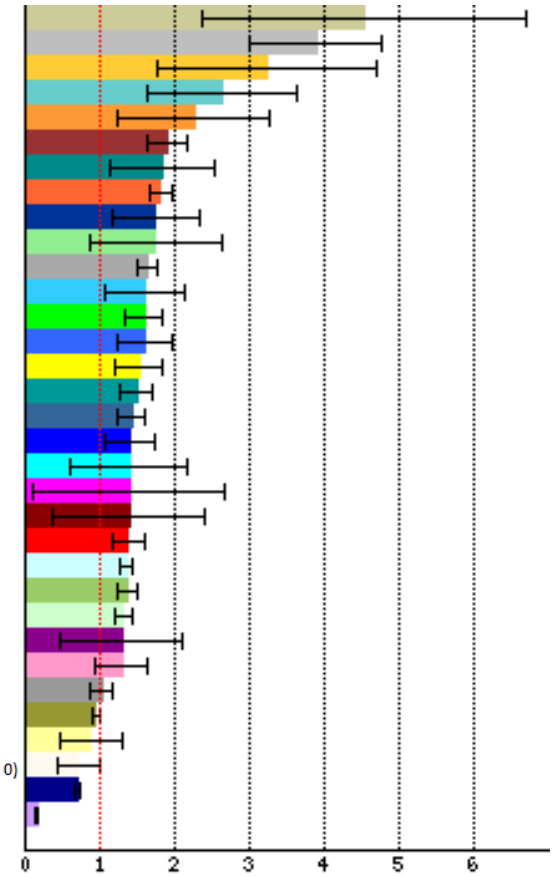

Fig. 2

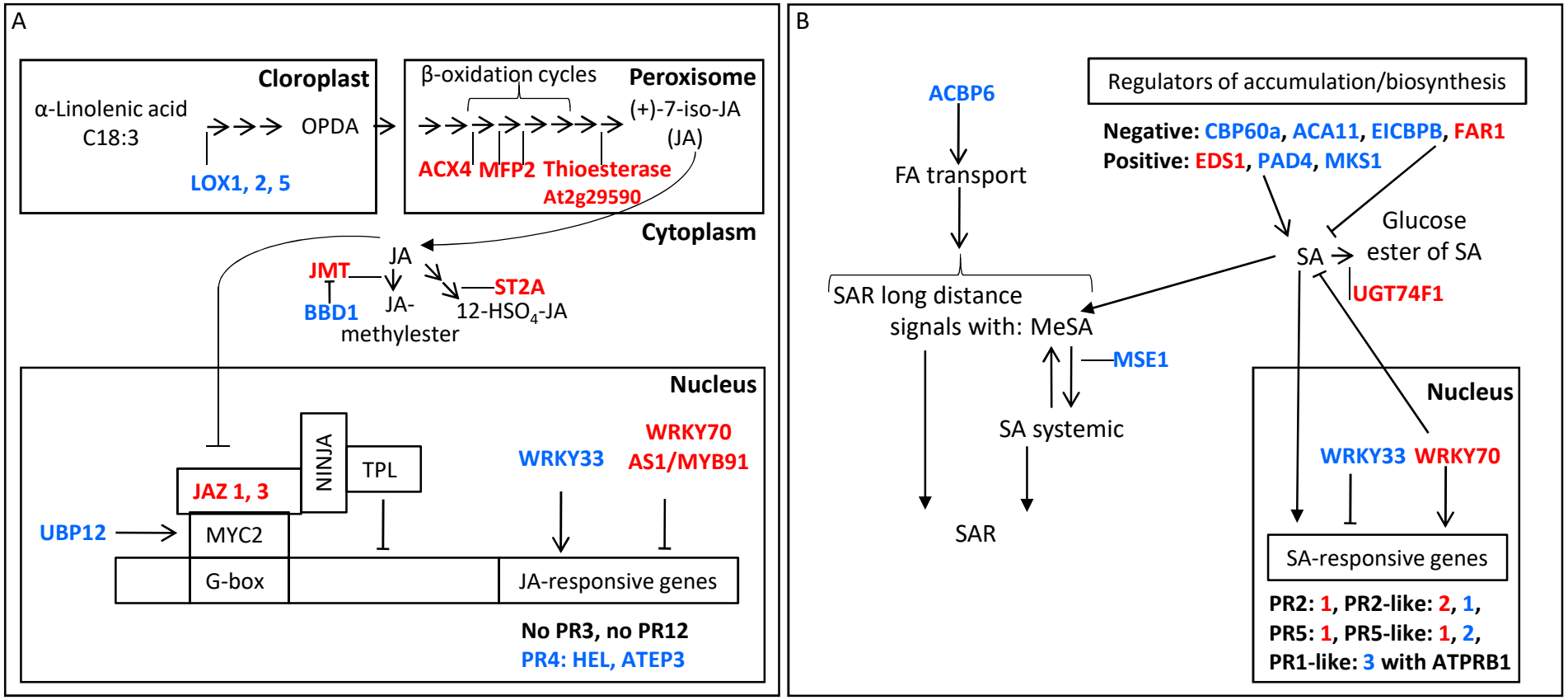
A
Cloroplast
α-Linolenic acid
C18:3
OPDA
LOX1, 2, 5
β-oxidation cycles
Peroxisome
(+)-7-iso-JA
(JA)
ACX4
MFP2
Thioesterase
At2g29590
Cytoplasm
JA
JMT
BBD1
JA-
methylester
ST2A
12-HSO4-JA
Nucleus
NINJA
TPL
JAZ 1, 3
UBP12
MYC2
G-box
WRKY33
WRKY70
AS1/MYB91
JA-responsive genes
No PR3, no PR12
PR4: HEL, ATEP3
B
ACBP6
FA transport
SAR long distance
signals with: MeSA
MSE1
SA systemic
SAR
Regulators of accumulation/biosynthesis
Negative: CBP60a, ACA11, EICBPB, FAR1
Positive: EDS1, PAD4, MKS1
SA
Glucose
ester of SA
UGT74F1
Nucleus
WRKY33
WRKY70
SA-responsive genes
PR2: 1, PR2-like: 2, 1,
PR5: 1, PR5-like: 1, 2,
PR1-like: 3 with ATPRB1

Fig. 3

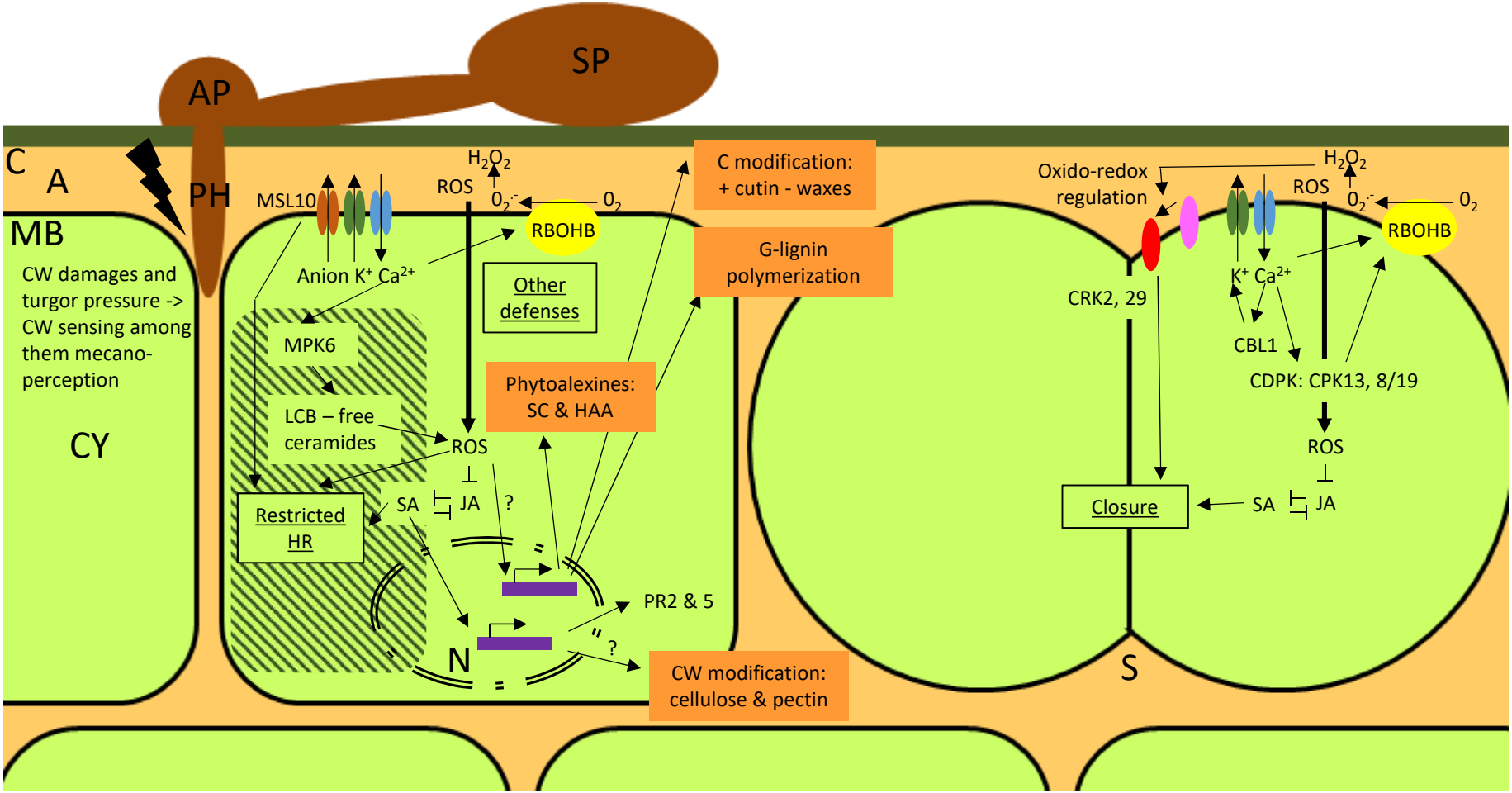
SP
AP
C
A
PH
MB
CW damages and turgor pressure -> CW sensing among them mecano-perception
CY
MSL10
Anion K+ Ca2+
MPK6
LCB – free ceramides
Restricted HR
ROS
H2O2
O2.-
O2
RBOHB
Other defenses
Phytoalexines: SC & HAA
SA
JA
?
N
PR2 & 5
C modification: + cutin - waxes
G-lignin polymerization
CW modification: cellulose & pectin
Oxido-redox regulation
CRK2, 29
K+ Ca2+
CBL1
CDPK: CPK13, 8/19
Closure
S

Fig. 4

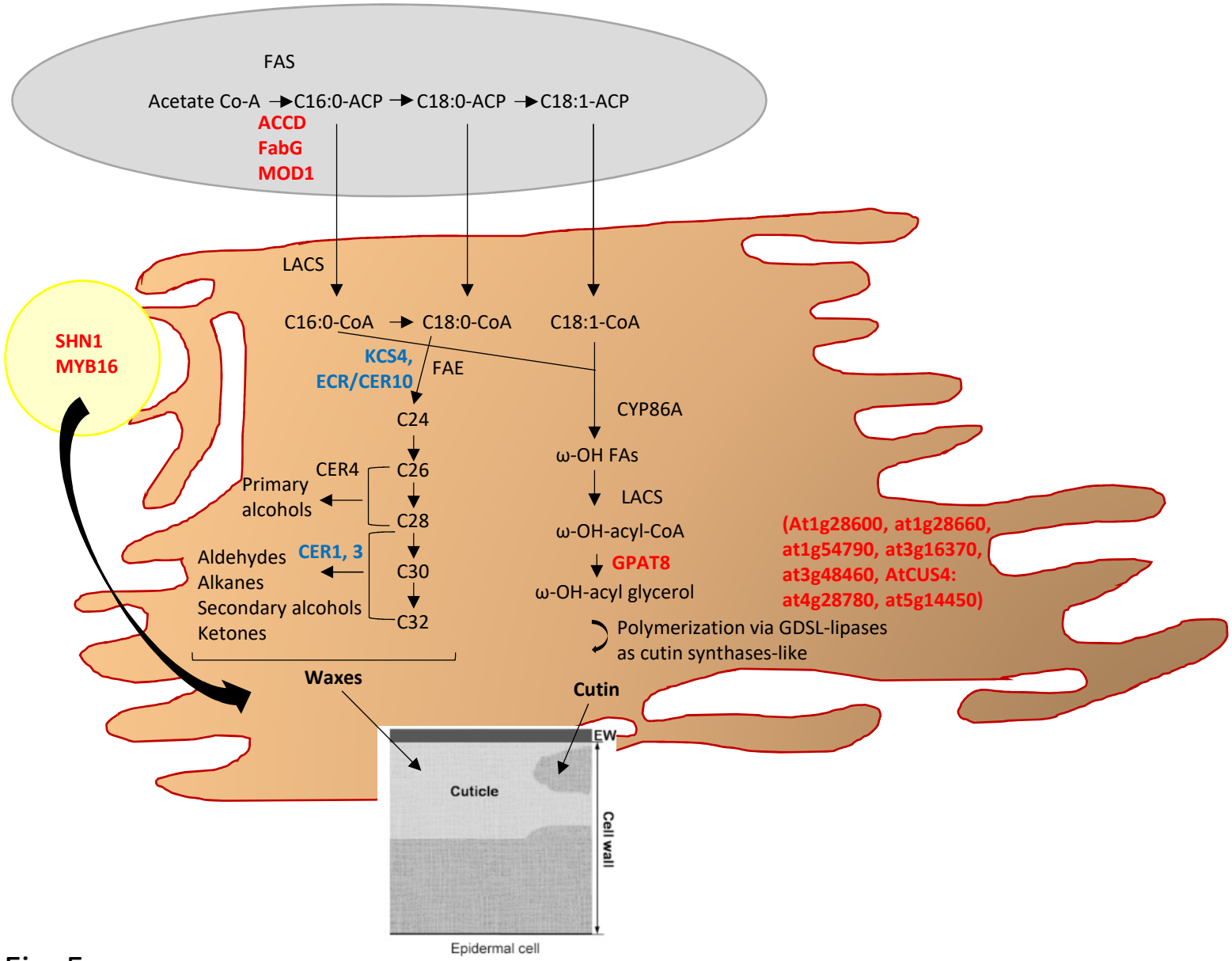
FAS
Acetate Co-A
C16:0-ACP
C18:0-ACP
C18:1-ACP
ACCD
FabG
MOD1
LACS
C16:0-CoA
C18:0-CoA
C18:1-CoA
KCS4,
ECR/CER10
FAE
C24
C26
C28
C30
C32
CER4
Primary alcohols
CER1, 3
Aldehydes
Alkanes
Secondary alcohols
Ketones
Waxes
CYP86A
ω-OH FAs
LACS
ω-OH-acyl-CoA
GPAT8
ω-OH-acyl glycerol
(At1g28600, at1g28660, at1g54790, at3g16370, at3g48460, AtCUS4: at4g28780, at5g14450)
Polymerization via GDSL-lipases as cutin synthases-like
Cutin
SHN1
MYB16
EW
Cuticle
Cell wall
Epidermal cell

Fig. 5

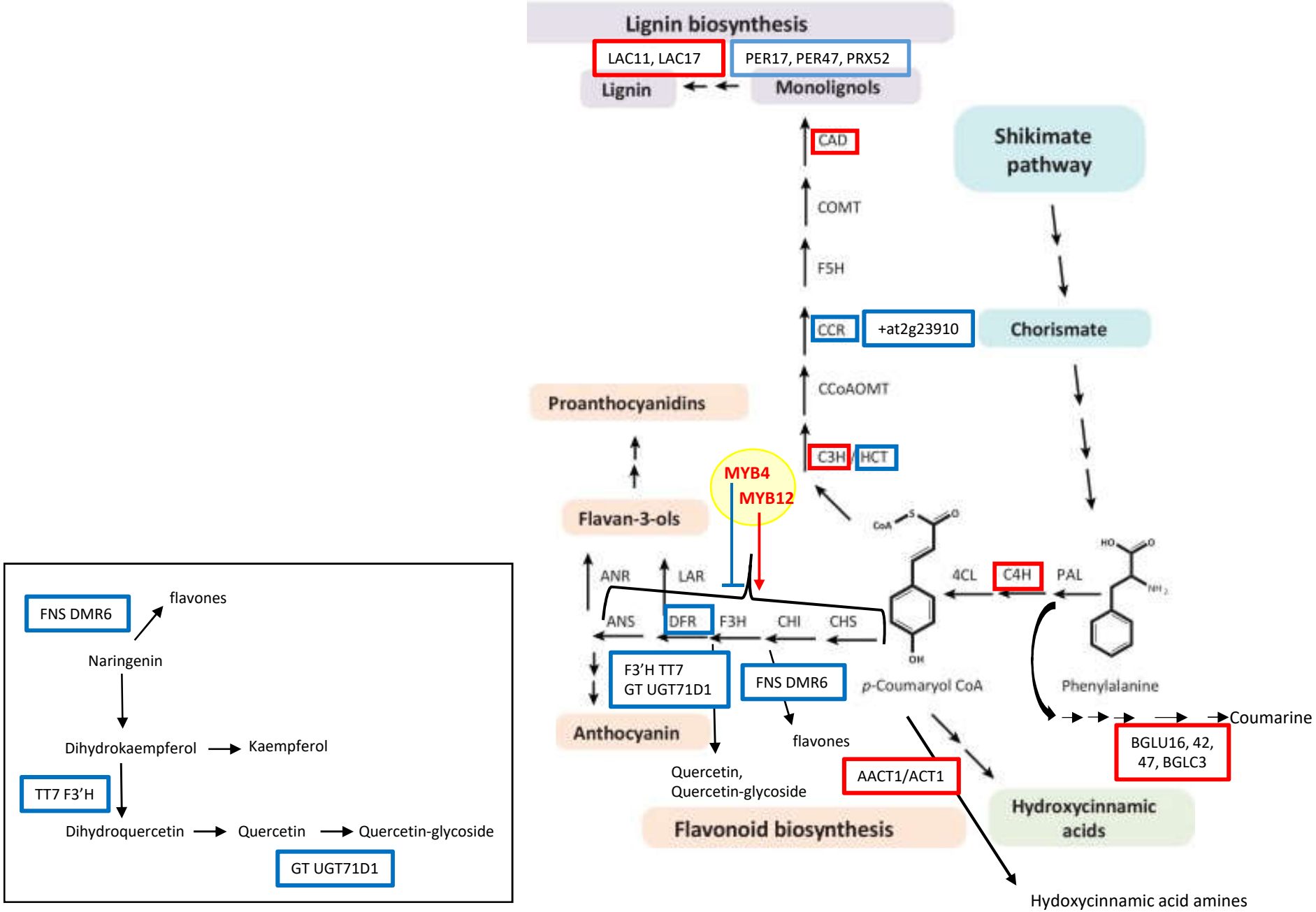
Lignin biosynthesis
LAC11, LAC17
PER17, PER47, PRX52
Lignin
Monolignols
CAD
COMT
F5H
CCR
+at2g23910
CCoAOMT
C3H
HCT
Shikimate pathway
Chorismate
Proanthocyanidins
MYB4
MYB12
Flavan-3-ols
ANR
LAR
ANS
DFR
F3H
CHI
CHS
4CL
C4H
PAL
F3'H TT7
GT UGT71D1
FNS DMR6
p-Coumaryol CoA
Phenylalanine
Coumarine
BGLU16, 42, 47, BGLC3
Anthocyanin
flavones
Quercetin, Quercetin-glycoside
AACT1/ACT1
Hydroxycinnamic acids
Flavonoid biosynthesis
Hydoxycinnamic acid amines
FNS DMR6
flavones
Naringenin
Dihydrokaempferol
Kaempferol
TT7 F3'H
Dihydroquercetin
Quercetin
Quercetin-glycoside
GT UGT71D1

Fig. 6